

Cylindrical manifolds in phase space as mediators of chemical reaction dynamics and kinetics. I. Theory

N. De Leon^{a)}

Department of Chemistry/Physics/Astronomy, Indiana University Northwest, Gary, Indiana 46408

Manish A. Mehta^{b),c)} and Robert Q. Topper^{d)}

Department of Chemistry, Yale University, New Haven, Connecticut 06518

(Received 29 January 1990; accepted 26 February 1991)

A microcanonical kinetic theory of reactions based upon the structure within phase space is developed. It is shown that the dynamics of reaction across an energetic barrier is mediated by invariant manifolds embedded in phase space that have the geometry of simple cylinders. The ideas are developed by considering molecular systems modeled by two vibrational degrees of freedom, a reaction coordinate and a "bath" coordinate. The kinetic theory is constructed by focusing on the dynamics between n mapping planes (" n -map") and the "reactive island" (RI) structure within them. We discuss how the structure of the conformer population decay in isomerization reactions can be obtained from the RI kinetic model. Formal solutions of the kinetic equations are discussed with specific attention given towards the calculation of the isomerization reaction rate. The formal theory is developed in Paper I of this series. Numerical considerations and applications to the reaction dynamics of model molecular systems with two degrees of freedom will be given in Paper II and extension of the theory and applications to multidimensional systems will be given in Paper III.

I. INTRODUCTION

An energetic barrier separating reactants from products must be overcome in order for most chemical reactions to proceed. A reactant molecule that has in some manner acquired enough energy to exceed the potential barrier is said to be *activated*. The experimental rate at which activated molecules become products is related to the concentration of reactants by the rate constant for the reaction. For example, in the unimolecular conversion $A \rightarrow B$ the rate of formation of B is given by $k_{A \rightarrow B} [A]$, where $k_{A \rightarrow B}$ is the rate constant and $[A]$ is the concentration of A .¹⁻⁵

Chemical reactions are typically classified as "complex" if they can be decomposed into two or more "elementary" reactions. Each elementary reaction has associated with it a set of well-defined rate constants. The resulting series of elementary steps, which give rise to the overall complex reaction, is then referred to as the kinetic mechanism. The overall rate law for the complex reaction is obtained from the first-order differential equations which arise from the kinetic mechanism.

From a theoretical perspective, it is desirable to be able to describe and understand the microscopic process of reactants becoming products. In other words, one would like to know the detailed dynamical pathways reactants must traverse to become activated and ultimately become products. The aggregation of such information is fundamentally a dynamical problem. Such a detailed description of the dynamics forces one to focus on the subprocesses within elementary

reactions. Thus, the goals of both of the above perspectives are similar in that an understanding of an overall reaction in terms of its constituent processes is sought.

The problem of calculating rates and rate constants for elementary reactions is one that has received considerable attention over the past several decades—the earliest studies being those of Eyring, Wigner, and Hirshfelder.^{6,7} Since those initial studies, a large body of literature on reaction rate theories has been established. For example Kramer first considered rates of reaction in viscous media.⁸ Rice–Ramsperger–Kassel (RRK) developed a simple statistical model of reaction rates based upon the complete randomization of the dynamics of N (harmonic) oscillators.^{2,3,5} Marcus modified the RRK statistical model to include the density of activated states and the density of transition states (RRKM).⁹⁻¹¹ Keck proposed variational transition state theory and discussed the least upper bound to the rate of bi- and ter-molecular reactions.¹² Light and Pechukas developed a phase space theory of chemical reaction rates.¹³⁻¹⁵ Miller developed the quantum and semiclassical version of transition state theory (TST) (Eyring theory).¹⁶ Miller, Pollak, Pechukas, and Child developed a phase space flux theory for bimolecular reactions.¹⁷⁻²⁰ Several other theoretical studies are also under development which seek to establish a unimolecular rate theory for molecular systems in the condensed and gas phase.²¹⁻²⁷ The statistical theories mentioned above have proven to be of fundamental value in both predicting and understanding chemical reaction rates. The reader interested in the recent developments and historical survey of reaction rate theories is referred to several excellent articles.^{20,28,29}

The fundamental nature of the above cited theories notwithstanding, experimental work and numerical models of chemical reactions reveal some basic discrepancies with the-

^{a)} Work performed at Yale University.

^{b)} NATO–NSF Postdoctoral Fellow.

^{c)} Present Address: Department of Theoretical Physics, University of Oxford, 1 Keble Road, Oxford, OX1 3NP.

^{d)} Present address: Department of Chemistry and Supercomputing Institute, University of Minnesota, Minneapolis, MN 55455-0431.

ory.^{30–40} Such disagreements have been especially well cited for unimolecular reactions. In some cases, the trends (pressure dependence, isotopic substitution, etc.) predicted by these theories are diametrically opposed to those observed. Such deviation between experiment and TST (or RRKM) theory is often referred to as “non-RRKM” behavior.

The development of a kinetic theory of reactions that accurately treats both the decay of initial nonequilibrium populations and the associated decay rates (rate constants), requires physical models that allow one to understand, from first principles, the nature of the processes through which reactants become products. Given a reasonably accurate potential energy surface, obtained through spectroscopic or *ab initio* means, one should be able not only to obtain reasonable agreement with experimental rate data, but also gain an understanding of precisely how and why a theoretical prediction may deviate from what is observed. It is precisely for this kind of detailed information that a significant amount of both theoretical and experimental work has been attempted.

The basic statistical theory that has emerged to describe unimolecular reactions is typically referred to as “RRKM” or “TST” theory. These theories are the most simple possible statistical theories that recognize the existence of a quantum (or classical) density of states. Perhaps Bauer states the situation best when he writes “*It [RRKM theory] is not an approximation to a realistic model; rather, it is an accurate solution to an idealized model.*”³⁴ An important question is then, under what conditions are the molecular dynamics not ideal?

The above question is one that was initially recognized by Wigner and Hirshfelder.⁷ In their classic paper they discuss the “recrossing” problem and how it may be dealt with in calculating quantum transmission coefficients, i.e., branching ratios. Miller focused on the recrossing problem and developed a unified statistical rate theory that bridged the gap between the rate theory for bimolecular reactions that are “direct” and the rate theory for bimolecular reactions that proceed through a long-lived complex.⁴¹ Pollak, Pechukas, Child, and J. P. Davis discussed how one may go beyond the unified statistical theory of Miller to solve the recrossing problem with less restrictive assumptions and thus develop a more accurate rate theory for bimolecular reactions.^{17–20,42–44}

Much of the focus of the above work has been to develop a rate theory that does not require explicit dynamical information. However, the studies of Pollak, Pechukas, Child, J. P. Davis, and Truhlar⁴⁵ have shown that an accurate treatment of the recrossing problem must include within it dynamical information. From the perspective of nonlinear dynamics this implies that the structure of phase space must be understood in some detail in order to develop an accurate rate theory.

M. J. Davis, Gray, and Skodje, in their studies of chemical reaction and intramolecular relaxation, demonstrated the necessity to understand the nonlinear dynamical underpinnings.^{46–51} Some of the earliest discussions along these lines were those of Pollak and Pechukas where they demonstrated that PODS [periodic orbit dividing surface(s)] were the natural dividing surfaces between reactants and prod-

ucts in collinear bimolecular reactions (e.g., $H + H_2 \rightarrow H_2 + H$). These authors went further to show that PODS were either “attractive” or “repulsive” in character.^{18–20} Pollak and Child went on to consider bimolecular reactions with a repulsive–attractive–repulsive PODS sequence and demonstrated that deviations from classical transition state theory were accounted for by “tubes” which emerge from the repulsive PODS.^{19,20} De Leon and Berne⁵⁰ and Gray and Rice⁵¹ considered unimolecular isomerization ($A \rightleftharpoons B$). Gray and Rice demonstrated that “turnstiles” arising from the standard homoclinic tangle could be used to understand isomerization reactions. M. J. Davis was able to show that “cantori” controlled the classical intramolecular relaxation of collinear OCS.⁴⁶ M. J. Davis, Skodje, and Gray demonstrated the utility of these cantori in understanding the failure of RRKM theory for the molecular systems $He + I_2$ and $I + HI$.^{47,48} M. J. Davis considered the map structure and homoclinic tangle of $H + H_2$.⁴⁹ It is interesting, indeed somewhat humbling, to note that much of the work above, especially with regard to PODS and reactive islands (see below) was anticipated in 1955 by De Vogelaere and Boudart.⁵²

While the current development of reaction rate theory is impressive, nevertheless it is apparent that some basic ideas regarding the details of reaction dynamics have yet to be developed and incorporated into a general reaction rate theory. In particular, a reaction rate theory that places the microscopic subprocesses within bimolecular and unimolecular reaction on an equal footing currently does not exist. One may naturally inquire why such a unification is important or even desirable? Aside from purely aesthetic reasons, the answer is that it is likely new principles will be learned in the course of such a unification.

In recent publications we focused our attention on the problem of unimolecular conformational isomerization and found dynamical structures we called “reactive islands” (RI). These reactive islands have the important property that all pre- or post-reactive motion must pass through them. A kinetic theory based upon the reactive islands was developed and accounted for non-RRKM behavior in model molecular systems.^{53,54} Since those initial publications we have shown that the nature of these reactive islands can be understood by focusing on the structure of four-dimensional phase space.⁵⁵ In so doing, one finds that the reactive islands are a direct consequence of the existence of invariant phase space manifolds embedded in four-dimensional phase space that have the geometry of simple cylinders. The intersection of Poincaré mapping surfaces with these cylinders generates the reactive islands. These results, including rudimentary aspects of what we call an “*n*-map” RI kinetic model and the relationship of reactive islands to the homoclinic tangle, was the focus of a recently submitted publication.⁵⁵

In this paper we develop in detail the fundamentals of the *n*-map RI kinetic theory and the cylindrical manifolds with emphasis on the problem of conformational chemical isomerization. The theory is formulated in terms of simple matrix equations which allow the direct calculation of conformer population decays and decay rates. Both numerical considerations and applications to specific molecular mod-

els with two degrees of freedom is left for Paper II of this series.⁵⁶ Extension of the theory and application to multidimensional molecular systems will be given in Paper III.⁵⁷ These introductory remarks would not be complete without stating that this work owes a significant debt to the pioneering efforts of Davis and co-workers⁴⁶⁻⁴⁹ in the field of nonlinear dynamics and its application to the problem of molecular relaxation.

This paper has been written with an intent that it be self-contained and present a logical progression in developing the theory. The "set theoretic" notation used throughout the text is not only necessary but an integral part of the overall theory. The reader interested in a detailed account of the theory is advised to read each section carefully—including frequent reference to the figures, before proceeding to the next section. Reference to our earlier papers would also be useful.⁵³⁻⁵⁵ The reader interested in a less detailed account of the theory is advised to read Secs. I and II and the discussion in Sec. VI.

The manuscript is arranged in the following manner: In Sec. II we discuss the cylindrical manifolds. In Sec. III we focus on how the cylindrical manifolds mediate the reaction dynamics and define n -map dynamics. In Sec. IV we develop the generalized RI kinetic theory for two- and multi-state isomerization. In Sec. V we discuss the solutions to the RI kinetic equations and focus on the calculation of the kinetic decay rate. In Sec. VI we discuss our results and conclusions.

II. CYLINDRICAL MANIFOLDS

A. General considerations

The dynamics of bimolecular reactions distinguishes itself from the dynamics of unimolecular isomerization in that motion in the former is unbound. Consequently, for bimolecular reactions one naturally focuses on the dynamical flux from asymptotic reactants to asymptotic products. This flux is then directly related to the reaction rate constant. The situation is, however, different for unimolecular isomerization. Motion that reacts from one conformer to another must recross the transition state. It is now less than straightforward to identify the asymptotic flux and thus the rate constant for the reaction.

The canonical rate constant, according to transition state theory, is proportional to the dynamical flux across the transition state. Thus

$$\text{Rate} \propto \text{Tr}(e^{-\beta H} |p_1 \delta(q_1 - q^\dagger)|), \quad (1)$$

where $\text{Tr}(\dots)$ is the classical trace and (q_1, p_1) are the reaction coordinate and momenta, respectively. A fundamental assumption of TST theory is that motion does not recross the dividing surface in a time scale short compared to the reaction time scale. This assumption can, under some situations, be a good approximation for bimolecular reactions. However for bound motion, recrossing of the dividing surface always occurs—typically in a short time scale relative to reaction. Thus, it is apparent that an accurate rate theory of isomerization must directly address the recrossing problem. To attack this problem at a microscopic level it is necessary to understand some basic ideas about the structure of phase space associated with chemical reaction.

B. Uncoupled motion

In a previous paper we developed the concepts of cylindrical manifolds in Hamiltonian systems, their properties and their role in mediating the dynamics across potential barriers.⁵⁵ In this section we consider the basic elements of that paper, focusing on those aspects most relevant to chemical reaction. Throughout this manuscript we will assume that the Hamiltonian for the molecular system is invariant to time reversal. Concepts in nonlinear dynamics and chaos will be used throughout this text. Several excellent books are available for the reader not familiar with this field.⁵⁸⁻⁶¹

Consider the reaction dynamics of a molecular system. We assume that reaction occurs across a potential barrier with a simple saddle at energy E_b . Let q_1 be the reaction coordinate and q_2 be a transverse "bath" coordinate. For simplicity we will assume that the transition state between states A and B will be at $q_1 = q^\dagger$, state A : $q_1 > q^\dagger$ and state B : $q_1 < q^\dagger$.

1. Unbound motion

It is convenient to first consider the situation when motion is not bound along the reaction coordinate and the two modes are uncoupled, Fig. 1. We let state A represent reactants and state B represent products. This system could serve as an approximate model for a bimolecular reaction (e.g., $\text{H} + \text{H}_2 \rightarrow \text{H}_2 + \text{H}$). We let the Hamiltonian be given by

$$H(\mathbf{p}, \mathbf{q}) = H_1(p_1, q_1) + H_2(p_2, q_2). \quad (2)$$

Motion generated by H can be considered as the composite dynamics of the two one dimensional subsystems H_1

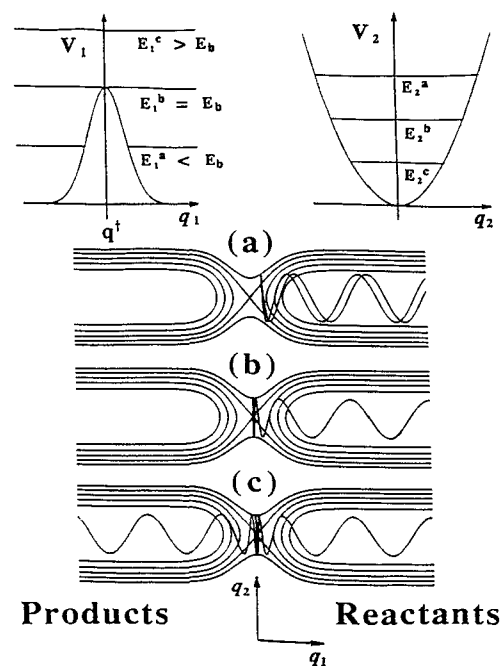


FIG. 1. Two state dynamics across a potential barrier. Three distinct situations are shown: (a) nonreactive, (b) asymptotic to τ , and (c) reactive trajectories. The upper left- and right-hand part of the figure represent one dimensional cuts of the potential along the reaction (q_1) and bath (q_2) coordinates, respectively. All three trajectories displayed are at the same total energy $E_1 + E_2 = E$ for a, b , and c .

and H_2 . However, it is instructive to examine the separable dynamics in full four-dimensional phase space. First, consider the structure of phase space at a total excess energy ΔE above E_b . The total energy may be partitioned in various ways between H_1 and H_2 : A reactant trajectory at $q_1 > q^\ddagger$ with $p_1 < 0$ and $E_1 < E_b$ will reflect off the barrier, going back towards reactants and never return, Fig. 1. In phase space the trajectory will lie on a two-dimensional invariant surface whose geometry is the direct product of the circular S^1 topology of the q_2 mode and the linear R^1 topology of the unbound reaction coordinate q_1 . The $R^1 \times S^1$ geometry corresponds to a simple cylinder. Motion on this invariant cylinder will have a constant action J_2 in the q_2 mode. [We will denote this invariant cylinder as $\Omega_{J_2}^A(E)$.] This cylinder is completely contained within the reactant side of the dividing surface q^\ddagger . A schematic drawing of the situation in phase space is given in Fig. 2. At a total energy E a continuous set of foliated cylinders $\Omega_{J_2}^A(E)$ will exist for all energies $E_1 < E_b$.

At $E_1 = E_b$ a reactant trajectory at $q_1 > q^\ddagger$ and with $p_1 < 0$ will approach the barrier top but will never quite reach it in the infinite future. Similarly a trajectory at $q_1 > q^\ddagger$ with $p_1 > 0$ will approach the barrier top but never quite reach it in the infinite past, Fig. 1. The first trajectory will lie on an invariant surface which we denote as $W_A^-(E)$ and the second trajectory will lie on an invariant surface $W_A^+(E)$. Both of these surfaces approach at the barrier top asymptotically and have the geometry of an open cylinder. In positive time motion on $W_A^+(E)$ is outgoing from the barrier top and motion on $W_A^-(E)$ is incoming to the barrier top. A similar pair of cylinders $W_B^\pm(E)$ will be embedded in the product phase space. The four cylinders, $W_A^+(E)$ and $W_B^\pm(E)$, meet at a periodic orbit $\tau(E)$ which lies along the barrier top cf. Fig. 2.

If $E_1 > E_b$ a reactive trajectory at $q_1 > q^\ddagger$ with $p_1 < 0$ will react and never return, Fig. 1. In this case the trajectory will

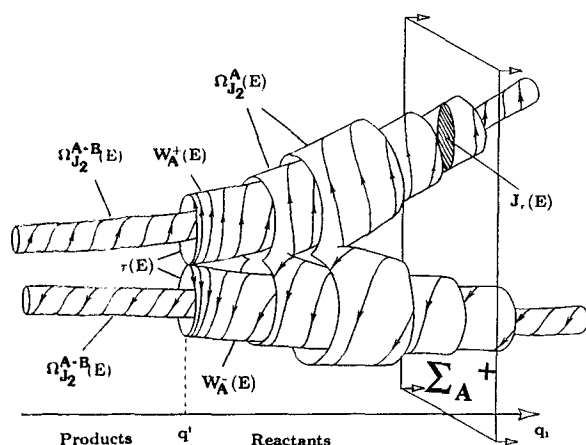


FIG. 2. Phase space invariant manifolds for the system in Fig. 1. The plane Σ_A is an oriented surface. The region shaded within the cylinder $W_A^+(E)$ is the symplectic area of the cylinder and is equal to the action of the periodic orbit τ . The "elbow" of the cylinder $\Omega_{J_2}^A(E)$ has been cut away to reveal the underlying foliated structure. The orbit labeled $\tau(E)$ is the periodic orbit at the transition state and thus represents the dividing line between reactants and products.

lie on an invariant cylinder $\Omega_{J_2}^{A \rightarrow B}(E)$ that crosses the barrier top, Fig. 1. A continuous set of foliated cylinders $\Omega_{J_2}^{A \rightarrow B}(E)$ will exist for reactive motion $A \rightarrow B$ at a total energy E . A similar set of foliated invariant cylinders on which reactive motion $B \rightarrow A$ will lie also exists and will be denoted by $\Omega_{J_2}^{B \rightarrow A}(E)$, Fig. 2.

The set of invariant cylinders

$$\{\Omega_{J_2}^A(E), \Omega_{J_2}^B(E), \Omega_{J_2}^{A \rightarrow B}(E), \Omega_{J_2}^{B \rightarrow A}(E), W_A^\pm(E), W_B^\pm(E)\}$$

then constitutes the complete phase space structure for this uncoupled system. A schematic drawing of the structure of the phase space for this situation is given in Fig. 2. The cylinders $W_A^\pm(E)$ and $W_B^\pm(E)$ represent the phase space boundary between reactive and nonreactive motion. Consequently, they represent the global separatrix to reaction for the system.

Having described the structure of phase space for the above uncoupled system, we consider two kinds of perturbations; (1) a perturbation which couples the two modes and (2) a perturbation which bounds the dynamics. We first consider bound motion.

2. Bound motion

Consider the dynamics between two potential wells separated by an energy barrier with a simple saddle. Assume that the two modes q_1 and q_2 are not coupled. What is the structure of phase space in this case? Locally about the saddle point, the potential looks the same as that of the unbound system. All invariant manifolds for the bound system must have the same local structure as those of the unbound system. We can again consider three separate energetic situations. For $E_1 < E_b$ the invariant cylinder we previously denoted $\Omega_{J_2}^A(E)$ will now close to form an invariant torus located within conformer A, Fig. 3. For $E_1 > E_b$ the open cylinders $\Omega_{J_2}^{A \rightarrow B}(E)$ and $\Omega_{J_2}^{B \rightarrow A}(E)$ will close to form an invariant torus that spans both conformers, $\Omega_{J_2}^{AB}(E)$, cf. Fig. 3. At $E_1 = E_b$ the cylinders $W_A^+(E)$ and $W_A^-(E)$ will close upon one another within conformer B, but remain open at $\tau(E)$. A similar situation occurs for conformer B. The resulting invariant manifolds, $W_A(E)$ and $W_B(E)$ will still

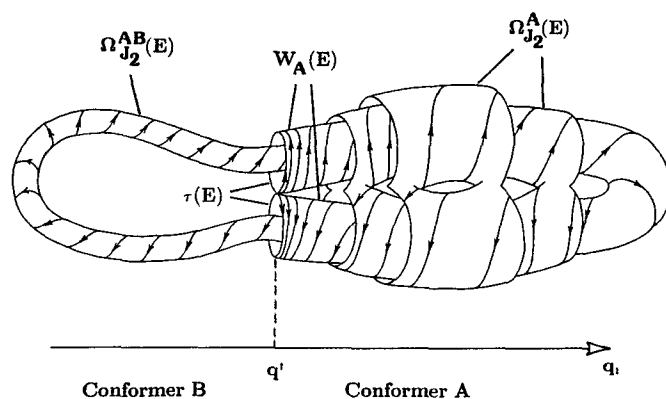


FIG. 3. Same as Fig. 2, except for bound motion. The invariant manifolds would in this case be associated with the dynamics of conformational isomerization. As in Fig. 2, the "ends" of the trapped tori have been cut away to reveal the underlying foliated structure.

have the geometry of a cylinder—open at the periodic orbit $\tau(E)$, Fig. 3. The cylinders $W_A(E)$ and $W_B(E)$, will meet and be “sewn” together at the periodic orbit $\tau(E)$. The manifold $W_A(E) \cup W_B(E)$ has the geometry of a torus, however this torus is decomposable since motion on W_A will never propagate onto W_B (i.e., $\phi, Z \notin W_B, \forall Z \in W_A$ and t, ϕ , is the dynamical propagator). A sketch of the foliated manifolds is given in Fig. 3.

The set of manifolds in Fig. 3 constitutes the complete phase space structure for uncoupled two state isomerization. The physical interpretation of the phase space structure is simple: Reactive motion must lie on invariant tori $\Omega_{J_2}^{AB}(E)$ and nonreactive motion must lie on tori $\Omega_{J_2}^A(E)$ or $\Omega_{J_2}^B(E)$. Since the system is uncoupled there is no possibility for interconversion between trapped and reactive motion. The cylinders $W_A(E)$ and $W_B(E)$ constitute the phase space boundary between reactive and trapped motion.

C. Poincaré maps

Before proceeding to the situation where the modes are coupled it is instructive to discuss the Poincaré map structure for the case of bound motion. To do so we consider the following Poincaré mapping surfaces

$$\begin{aligned}\Sigma_{q_2}^{\pm} &= \{Z \in \Gamma, q_2 = q_2^0, \pm p_2\}, \\ \Sigma_{q_1}^{\pm} &= \{Z \in \Gamma, q_1 = q_1^0, \pm p_1\},\end{aligned}\quad (3)$$

where Γ is the set of phase space points in R^4 phase space and q_k^0 is some fixed value of q_k . The set of isoenergetic points on a Poincaré map will be denoted by $\Sigma_q^{\pm}(E)$,

$$\begin{aligned}\Sigma_{q_2}^{\pm}(E) &= \Sigma_{q_2}^{\pm} \cap H_E, \\ \Sigma_{q_1}^{\pm}(E) &= \Sigma_{q_1}^{\pm} \cap H_E,\end{aligned}\quad (4)$$

where H_E is the set of points ($Z \in \Gamma$) on the constant energy hypersurface $H(Z) = E$. How will these mapping planes slice the invariant manifolds in Fig. 3? The answer is clear, $\Sigma_{q_1}^+(E)$ will slice all the invariant manifolds revealing a dense set of concentric closed curves. Each curve is, of course, associated with an orbit in H_2 , Fig. 4(b). On the other hand $\Sigma_{q_2}^+(E)$ will result in the dense set of closed curves shown in Fig. 4(a). Each of these curves is associated with an orbit in H_1 . Note in particular the separatrix in the form of a “figure eight” in Fig. 4(a). The Poincaré mapping

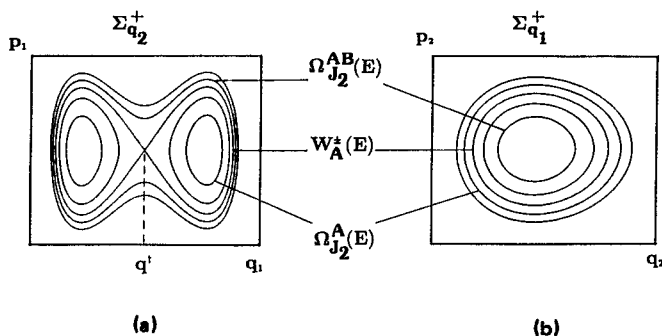


FIG. 4. Level curves at a total energy E for the two Poincaré maps; (a) $\Sigma_{q_2}^+$ and $\Sigma_{q_1}^+$ at a total energy E for the uncoupled bound state system in Fig. 3.

surface $\Sigma_{q_2}^+(E)$ slices $W_A(E) \cup W_B(E)$ along the cylindrical axis resulting in the figure eight pattern.

D. Coupled motion

We are now in position to consider perturbations which couple the modes. To see how a generic coupling affects the phase space structure it is necessary to focus on the periodic orbit $\tau(E)$. This periodic orbit is unstable regardless of the nature of the coupling. Stable and unstable manifolds will emerge from $\tau(E)$.⁶⁰ In general, periodic orbits give rise to stable and unstable manifolds which assume one of three possible geometries: a simple $R^1 \times S^1$ cylinder, a Mobius strip or a cylinder with one or more full twists homeomorphic to a simple cylinder.⁵⁵ Manifolds with the latter two geometries will cause nearby orbits to cross $\tau(E)$ in configuration space as they fall away. On the other hand, if the manifolds have the geometry of simple cylinders, then nearby orbits will fall away without recrossing τ in configuration space. The above described character of nearby orbits to τ has been previously discussed by Pollak, Pechukas, and Child. They have classified periodic orbits in the following way: if orbits nearby $\tau(E)$ recross τ while falling away, then $\tau(E)$ is called “attractive.” If nearby orbits do not recross $\tau(E)$ as they fall away then $\tau(E)$ is called “repulsive.”²⁰ Thus, if $\tau(E)$ is repulsive, then the stable and unstable manifolds generated from $\tau(E)$ will have an $R^1 \times S^1$ geometry. We will assume that when the modes are coupled $\tau(E)$ continues to be repulsive.⁶²

Four cylinders will be generated about $\tau(E)$: two stable $W_A^-(E)$, $W_B^-(E)$ and two unstable $W_A^+(E)$, $W_B^+(E)$. The cylinders $W_A^{\pm}(E)$ will extend into the phase space of conformer A and $W_B^{\pm}(E)$ will extend into the phase space of conformer B. When the modes are coupled the cylinders $W_A^+(E)$ and $W_A^-(E)$ will only *partially* overlap one another, Fig. 5. Each cylindrical manifold is a two-dimensional surface embedded in R^4 . Therefore the intersection of two cylindrical manifolds will occur along lines. Each of these

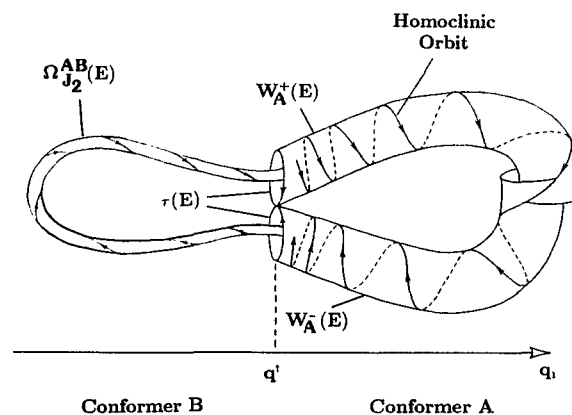


FIG. 5. Schematic drawing of two cylindrical manifolds generated from τ and embedded in phase space, for a generic coupled system. The two dimensional manifolds will overlap one another along one dimensional lines. These lines correspond to homoclinic orbits to τ . The small thin tube spanning both conformers corresponds to an invariant torus $\Omega_{J_2}^{AB}(E)$ that survives the coupling. The overlap volume is the region of phase space for which post reactive motion undergoes direct back reaction.

lines must asymptotically approach $\tau(E)$ along $W_A^+(E)$ and $W_A^-(E)$. Consequently, these lines must be homoclinic orbits, cf. Fig. 5.

To further understand these cylindrical manifolds within the context of nonlinear dynamics we consider the effect of their partial overlap on the observed structure of the Poincaré maps $\Sigma_{q_2}^+$ and $\Sigma_{q_1}^+$ in Fig. 4. On $\Sigma_{q_2}^+(E)$ the separatrix, which previously was a figure eight, will now be a tangled structure resulting from the intersections of $W_A^-(E)$ and $W_A^+(E)$ at homoclinic points. The resulting map structure is usually referred to as the homoclinic tangle, Fig. 6(a).⁶³ Note that the homoclinic oscillations must encroach upon regions of phase space that, in the uncoupled system, contained invariant tori. Consequently, invariant tori localized about the separatrix for the uncoupled system are destroyed in the coupled system resulting in dynamical chaos about the cylinders $W_A^+(E)$ and $W_B^+(E)$. A distinct situation arises on the $\Sigma_{q_1}^+(E)$ Poincaré map. As the cylinders $W_A^+(E)$ extend away from τ , their initial intersection with $\Sigma_{q_1}^+$ will result in two closed curves which may overlap one another. We have referred to these closed curves as "reactive islands" (RI).⁵³⁻⁵⁵ One can view the interior of the reactive islands as forward and backward propagation of the transition state phase space onto Poincaré mapping planes. However, we do not consider this viewpoint particularly useful as it does not address the boundary of the reactive island nor does it add to our understanding of the nonlinear dynamics.

The Poincaré map $\Sigma_{q_1}^+$ slices the cylindrical manifolds $W_A^+(E)$ along the S^1 topological circuit whereas the map $\Sigma_{q_2}^+$ slices the cylinders along the transverse R^1 (cylindrical axis) topological circuit. Thus, the two Poincaré maps in Figs. 4 and 6 contain distinct but complementary information about the phase space structure. It is interesting to note that if the coupling between the two modes is sufficiently strong, then it is possible that the map structure on $\Sigma_{q_2}^+(E)$ will be discontinuous, that is the stable and unstable branches on the Poincaré map will break up on the energetic periphery (cf. Fig. 4, Ref. 54). The possibility then exists that the map structure on $\Sigma_{q_2}^+(E)$ will contain reactive islands rather than the standard homoclinic tangle.⁵⁸⁻⁶⁰ This situation was in fact observed in earlier papers.^{53,54} This re-

sult is understood by noting that the cylinders $W_A^+(E)$ and $W_B^+(E)$ can wander away from the mapping plane $\Sigma_{q_2}^+$ before intersecting it again.⁵⁵

The generic structure of phase space for the bound coupled system at a total energy E can now be constructed. Invariant tori which reside completely in either side of $\tau(E)$ [i.e., $\Omega_{J_2}^A(E)$ and $\Omega_{J_2}^B(E)$] may exist, however, the measure of phase space that they consume will depend upon both the strength of the coupling and the energy E . Motion on these tori will, of course, never cross the barrier. Invariant tori which span both conformers may also exist [i.e., $\Omega_{J_2}^{AB}(E)$] (cf. Fig. 5). Motion on $\Omega_{J_2}^{AB}(E)$ will periodically cross the barrier. There will be a sea of chaos between the above two sets of invariant tori. The invariant cylinders $W_A^+(E)$ and $W_B^+(E)$, which are not compact manifolds,⁶⁴ will wind about the chaotic phase space indefinitely—continuously deforming and intersecting one another along a denumerably infinite set of homoclinic orbits to $\tau(E)$. This interweaving of the cylinders in phase space is the phase space homoclinic tangle.⁶⁵ It is within the chaotic phase space visited by the cylindrical manifolds $W_A^+(E)$ and $W_B^+(E)$ that molecular motion can become trapped, undergo trapped \rightarrow reactive motion and back react (recross the dividing surface). The manner in which the invariant cylinders overlap one another in phase space mediates the chemical reaction dynamics.

E. Phase space symmetry of cylinders

It is important to point out that the cylinders $W_A^+(E)$ and $W_A^-(E)$ are simply related to one another if the Hamiltonian dynamics has time reversal symmetry. To make this symmetry relation precise we can define the cylinders $W_A^\pm(E)$ as the set of points $Z^\pm \in \Gamma$ that asymptotically approach the periodic orbit $\tau(E)$ in the infinite future or past, i.e.,

$$\begin{aligned} W_A^-(E) &= \{Z^- : Z \in \Gamma, H(Z_t) = E, \\ &\quad (Z_{t \rightarrow +\infty} \in \Gamma_A) \rightarrow \tau(E)\}, \\ W_A^+(E) &= \{Z^+ : Z \in \Gamma, H(Z_t) = E, \\ &\quad (Z_{t \rightarrow -\infty} \in \Gamma_A) \rightarrow \tau(E)\}. \end{aligned} \quad (5)$$

Now let O_p be the momentum reversal operator, i.e., $O_p(\mathbf{p}, \mathbf{q}) = (-\mathbf{p}, \mathbf{q})$. If the dynamics has time reversal symmetry then $Z^- = O_p Z^+$. In other words, the cylinder $W_A^-(E)$ may be constructed from the cylinder $W_A^+(E)$ by taking all points $Z \in W_A^+(E)$ and reversing the momenta.

F. Cylinder mediated reaction dynamics

Having established the generic structure of phase space associated with coupled two state isomerization, we can use this insight to understand the reaction dynamics. Consider the cylinders $W_A^+(E)$ and $W_A^-(E)$ locally about the periodic orbit $\tau(E)$, Fig. 7(a). Motion on the cylinder $W_A^-(E)$ will asymptotically approach $\tau(E)$ but, of course, never quite reach it. Motion just exterior to $W_A^-(E)$ will also approach τ but will eventually fall back within conformer A .

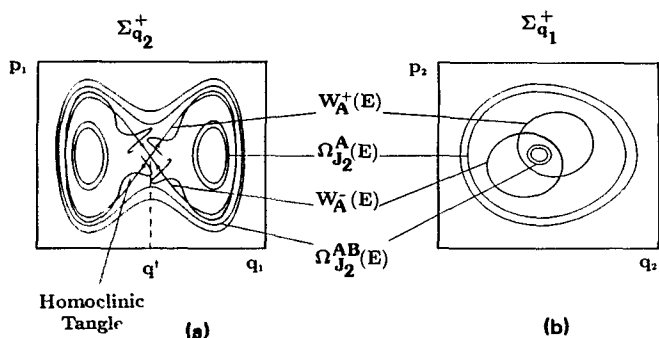


FIG. 6. Same as Fig. 4 except the two modes are coupled. Note the homoclinic tangle in (a). In (b) the reactive islands partially overlap. Note the invariant tori, $\Omega_{J_2}^{A-B}$, associated with regular reactive motion are located within the overlap region between the two reactive islands.

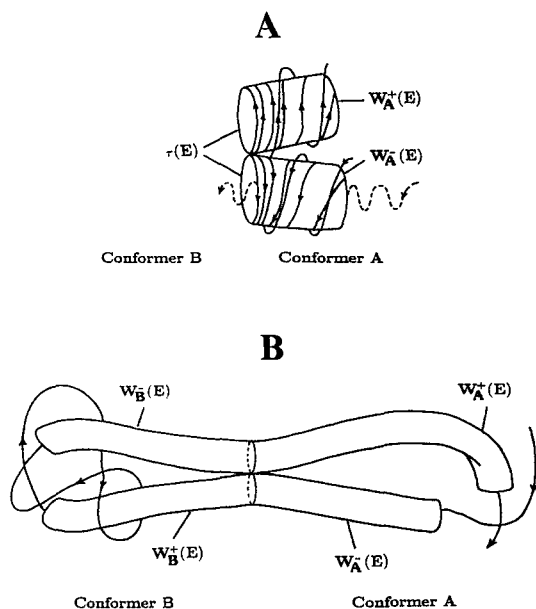


FIG. 7. Cylindrical manifolds embedded in phase space. In (A) motion local to τ is shown. In (B) the cylinders are seen to extend away from τ and thus are a global separatrix to reaction. The curve entering and exiting the cylinders represents a trajectory undergoing reaction.

On the other hand, motion just interior to $W_A^-(E)$ will approach $\tau(E)$ and eventually react onto conformer B. Therefore, all reactive motion $A \rightarrow B$ must pass through the interior of $W_A^-(E)$. On the other hand all reactive motion $B \rightarrow A$ will pass through the interior of $W_B^-(E)$.

The conclusions above are not restricted to motion local to $\tau(E)$. All motion on $W_A^-(E)$ will asymptotically approach $\tau(E)$. Consequently the cylinder $W_A^-(E)$ will serve as a global separatrix between “trapped” and reactive motion, Fig. 7(b).⁶⁶ The cylinder $W_A^-(E)$ has the important physical property of mediating all *pre-reactive* motion $A \rightarrow B$. Similarly, $W_B^-(E)$ has the physical property of mediating pre-reactive motion $B \rightarrow A$. On the other hand, due to time symmetry, $W_A^+(E)$ mediates *post-reactive* motion (i.e., motion which has just reacted) from $B \rightarrow A$ and $W_B^+(E)$ mediates post-reactive motion $A \rightarrow B$ respectively. Therefore, the four cylinders $W_A^\pm(E)$ and $W_B^\pm(E)$ mediate all pre- and post-reactive motion. These pre- and post-reactive cylinders can be numerically generated for specific Hamiltonian systems. In Fig. 8 we show a set of pre- and post-reactive cylinders and a trajectory generated for a particular Hamiltonian system representing conformational isomerization.^{54,55} The trajectory in Fig. 8 reacts from conformer A onto conformer B. Note how this trajectory enters the interior of $W_A^-(E)$ prior to reacting, winds about within $W_A^-(E)$ and finally reacts through $W_B^+(E)$.

All of the conclusions above are exact. Our objective is now to use the properties of the phase space manifolds to construct a kinetic theory of isomerization. The development of this kinetic theory is the subject of the rest of this paper.

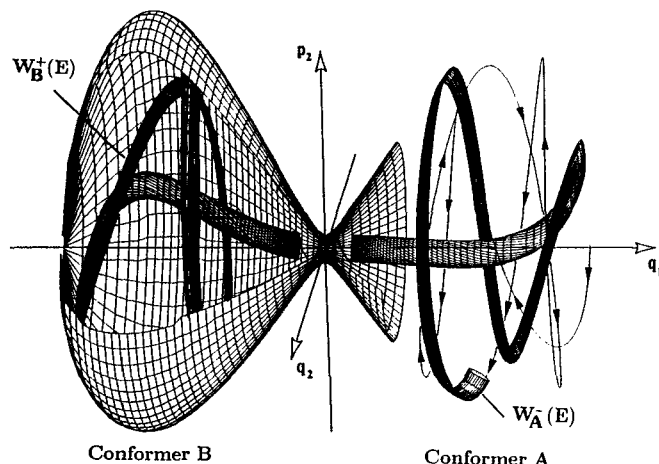


FIG. 8. A numerical reconstruction of the $W_A^-(E)$ and $W_B^+(E)$ cylindrical manifolds in the (q_1, q_2, p_2) axis and $H = E$. All dynamics is within the energetic boundary (“basket”) for a two degree of freedom Hamiltonian with highly coupled modes (Ref. 56). The calculation is at a total energy slightly above the barrier. Included in the figure is a numerically generated trajectory that is initially trapped in conformer A and eventually enters the interior of the cylinder $W_A^-(E)$ and thus reacts. Upon reaction the trajectory enters $W_B^+(E)$.

III. THE n -MAP AND REACTIVE ISLAND MEDIATED REACTION DYNAMICS

A. Two state dynamics

In two previous papers we considered reactive islands on a $\Sigma_{q_2}^+$ Poincaré map and developed a kinetic theory based upon on those maps. However, further work and the realization of the existence of the cylindrical manifolds has revealed that a more general kinetic theory can be developed based upon the map dynamics between multiple mapping surfaces we will call the n -map.

The existence of the $W_A^+(E)$ and $W_A^-(E)$ cylindrical manifolds and the property that they precisely mediate the reaction dynamics suggests that an accurate kinetic theory based upon these manifolds should be possible. Our goal in this section is to develop the necessary concepts to construct such a theory for two state conformational isomerization. With the concepts developed, the extension to more general cases (i.e., multiple conformational states) is straightforward (Sec. IV B).

Conventionally, one would view the relaxation of an initial nonequilibrium population distribution as a continuous function of time. A temporal kinetic theory of the relaxation process would naturally emerge. However, the properties of the phase space cylinders can most simply be exploited by conducting what we *n-map* rather than *temporal* dynamics.

Consider a system with two conformational states A and B for which we define two Poincaré maps as $\Sigma_A^+ = \Sigma_{q_1 > q^+}^+$ and $\Sigma_B^- = \Sigma_{q_1 < q^+}^-$ [cf. Eq. (3)]. The surfaces Σ_A^+ and Σ_B^- are oriented maps consisting of the bath coordinate and momentum (q_2, p_2) . Figure 6(b) is a typical example of the initial encounter of $W_A^\pm(E)$ with Σ_A^+ .

1. State A bound, state B unbound

We are now in position to describe the details of the microcanonical reaction dynamics and cylinder mediated kinetics. To make the forthcoming discussion as simple as possible, let us assume that state B is unbound and the cylinders $W_B^\pm(E)$ do not overlap one another (i.e., motion $A \rightarrow B$ never returns). This assumption will simplify the forthcoming discussion as we will not have to be concerned with recrossing motion from state B . We will relax this condition later. Also, let us assume that invariant tori $\Omega_A^+(E)$ are absent.

Intra- and inter-mappings of a point $Z \in (\Sigma_A^+ \text{ or } \Sigma_B^-)$ will occur between these two Poincaré surfaces. The dynamics between the two surfaces is then the map analogue to the temporal dynamics. The “map dynamics” is determined in the following manner: A point $Z \in \Sigma_A^+$, together with the total energy, uniquely specifies a trajectory. Hamilton’s equations of motion allow us to propagate Z : if Z_t propagates back onto Σ_A^+ then we know that during the course of its evolution Z_t did not cross the dividing surface. (If Z_t had crossed the dividing surface at q^\ddagger , then it must enter the interior of $W_B^+(E)$ and, in this case, never return.) The propagation of Z can be continued indefinitely. If Z_t maps onto Σ_A^+ , then it is propagated once again. In this manner Z_t is propagated on Σ_A^+ until it crosses the dividing surface and maps onto Σ_B^- . Such a sequence of mappings between Σ_A^+ and Σ_B^- is an example of 2-map dynamics.

Somewhat more formally, the 2-map dynamics is defined by the mapping $U: (\Sigma_A^+, \Sigma_B^-) \rightarrow (\Sigma_A^+, \Sigma_B^-)$ and time “ t ” is replaced by map iteration “ p ” generated by U . Since the mapping U is generated by Hamilton’s equations of motion then its inverse inverse U^{-1} , i.e., negative time dynamics, is well defined. The mapping sequence of a single trajectory Z_t beginning on Σ_A^+ will consist of K_Z mappings U onto Σ_A^+ . K_Z is then the “lifetime” of Z in state A .

The single point dynamics discussed above is easily extended to include an ensemble of M points $Z_j \in \Sigma_A^+$, $j = 1, 2, \dots, M$. Given such an ensemble there will be M mapping sequences within Σ_A^+ , the j th sequence consisting of K_j mappings onto Σ_A^+ . In this way one can count the number of points Z that remain in Σ_A^+ after the p th map iteration U^p of the ensemble. This number is then the population decay of state A as a function of p . The resulting population decay can be structured (i.e., not be a simple exponential decay) and is closely related to its temporal analogue. The structure and decay rate of the 2-map population decay can be understood and kinetically modeled with the cylindrical manifolds $W_A^\pm(E)$ and the manner in which they overlap with one another in phase space.

To develop the kinetic model we focus on the details of how a point $Z \in \Sigma_A^+$ becomes reactive. Previously we have noted that if motion is to react from state A to state B it must do so through the cylinder $W_A^-(E)$. The intersection of $W_A^-(E)$ with Σ_A^+ generates a reactive island whose area is equal to the action, $J_r(E)$, of the periodic orbit $\tau(E)$. Let the set of points Z within the reactive island bounded by this curve be denoted by Π_A^- , then

$$\Pi_A^- = \{Z: Z \in \Sigma_A^+(E), UZ \in \Sigma_B^-(E)\}. \quad (6)$$

The reactive island Π_A^- contains the *complete* set of pre-reactive points within $\Sigma_A^+(E)$, i.e., all points within $\Sigma_A^+(E)$ that react in the next mapping U must be a member of Π_A^- . An obvious consequence is that a point $Z \in \Sigma_A^+(E)$ cannot react unless it first maps onto Π_A^- . Similarly, the cylinder $W_A^+(E)$ will form a closed curve upon extension onto $\Sigma_A^+(E)$. Let the set of points Z within this reactive island be denoted by Π_A^+ , then

$$\Pi_A^+ = \{Z: Z \in \Sigma_A^+(E), U^{-1}Z \in \Sigma_B^-(E)\}. \quad (7)$$

Points $Z \in \Pi_A^+$ consist of the *complete* set of points $Z \in \Sigma_A^+(E)$ that are post-reactive. The preimage of all points $Z \in \Pi_A^+$ must lie on $\Sigma_B^-(E)$ [i.e., $U^{-1}Z \in \Sigma_B^-(E)$, $\forall Z \in \Pi_A^+$].

It is possible for the sets Π_A^- and Π_A^+ to have no points in common, i.e., $\Pi_A^- \cap \Pi_A^+ = \emptyset$. However, let us first consider the situation where $\Pi_A^- \cap \Pi_A^+ \neq \emptyset$, cf. Fig. 6(b). We will denote this common overlap region as Π_A ,

$$\begin{aligned} \Pi_A &= \Pi_A^+ \cap \Pi_A^- \\ &= \{Z: Z \in \Sigma_A^+(E), U^{\pm 1}Z \in \Sigma_B^-(E)\}. \end{aligned} \quad (8)$$

Therefore Π_A contains the *complete* set of points in $\Sigma_A^+(E)$ that have just reacted from state B and are just about to react onto state B (i.e., the complete set of points in $\Sigma_A^+(E)$ that are both pre- and post-reactive). A post-reactive trajectory Z_t mapping onto the overlap region Π_A will map onto $\Sigma_A^+(E)$ only once before recrossing the dividing surface—we will refer to such motion as *direct* back reaction. The fraction of motion which will undergo direct back reaction is easily obtained. Let $\text{Area}(\dots)$ denote the symplectic area of the set (\dots) . Then the fraction of post-reactive motion from state B that will undergo direct back reaction is given by [see Fig. 6(b)],

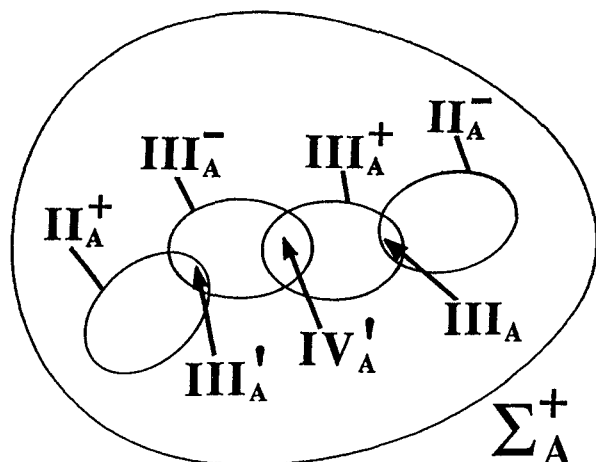
$$\begin{aligned} \text{Fraction of post-reactive} \\ \text{motion undergoing direct} &= \frac{\text{Area}(\Pi_A)}{J_r(E)}. \end{aligned} \quad (9)$$

back reaction

If $\Pi_A = \emptyset$, then direct back reaction is not dynamically possible. In this case the cylinders $W_A^\pm(E)$ will continue to evolve within the phase space of the conformer A and intersect $\Sigma_A^+(E)$ again—generating another set of reactive islands. A schematic depiction of one possible configuration of these reactive islands on $\Sigma_A^+(E)$ is shown in Fig. 9. Let the reactive islands so generated on $\Sigma_A^+(E)$ be denoted by III_A^+ and III_A^- . The reactive islands III_A^\pm contain the complete set of points that will react in two and only two backward or forward map iterations U , respectively,

$$\begin{aligned} \text{III}_A^+ &= \{Z: Z \in \Sigma_A^+(E), U^{-1}Z \in \Pi_A^+\} \\ &= U(\Pi_A^+), \\ \text{III}_A^- &= \{Z: Z \in \Sigma_A^+(E), UZ \in \Pi_A^-\} \\ &= U^{-1}(\Pi_A^-). \end{aligned} \quad (10)$$

Therefore, reactive islands III_A^- and Π_A^+ are the preimages of Π_A^- and III_A^+ . If $\text{III}_A = \text{III}_A^+ \cap \Pi_A^- \neq \emptyset$ (cf. Fig. 9), then the simplest route to back reaction will consist of a post-reactive trajectory undergoing two map iterations in $\Sigma_A^+(E)$, cf. Fig. 9. In this particular case,



$$\begin{aligned} \text{III}_A^+ &= U(\text{II}_A^+) \\ \text{II}_A^- &= U(\text{III}_A^-) \end{aligned}$$

FIG. 9. Schematic of the reactive islands generated on the conformer A map Σ_A^+ for primary-2 back reaction. The symplectic area associated with each reactive island is equal to $J_r(E)$.

Fraction of post-reactive

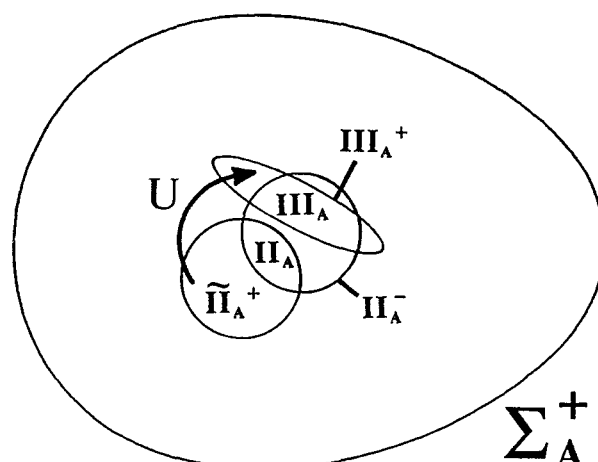
$$\text{motion undergoing two map} = \frac{\text{Area}(\text{III}_A)}{J_r(E)}. \quad (11)$$

iterations prior to
back reaction

Clearly, the above can be generalized: If $\text{III}_A = \emptyset$ then reactive islands IV_A^\pm will be generated by the cylinders. If $\text{IV}_A = \text{IV}_A^+ \cap \text{IV}_A^- \neq \emptyset$ then the simplest pathway for post-reactive motion to back react will consist of three map iterations on $\Sigma_A^+(E)$. To generalize: if the simplest pathway to back reaction consists of F mappings on $\Sigma_A^+(E)$ then we will call this route to back reaction "primary- F " back reaction. There will be $2F$ reactive islands on $\Sigma_A^+(E)$ whose symplectic area is equal to $J_r(E)$ and are denoted by $\text{II}_A^\pm, \text{III}_A^\pm, \dots, (F+1)_A^\pm$. The overlap region between $(F+1)_A^+$ and II_A^- is denoted by $(F+1)_A$. Then,

$$\text{Fraction of post-reactive} \\ \text{motion which undergoes primary-} F = \frac{\text{Area}((F+1)_A)}{J_r(E)}. \quad (12)$$

The discussion above has focused on the simplest route to back reaction. However, a detailed account of the reaction dynamics must be able to account for more complex back reactive pathways. Note that the overlap region associated with primary- F back reaction is bounded by homoclinic orbits. A denumerable but infinite set of homoclinic orbits exists thus implying an infinity of higher order pathways to back reaction. To see how these pathways may be accounted for, consider a situation where the overlap $\text{II}_A \neq \emptyset$. We decompose II_A^+ into the union of the overlap region II_A and its complement $\tilde{\text{II}}_A^+$, i.e., $\tilde{\text{II}}_A^+ = \text{II}_A^+ - \text{II}_A$, cf. Fig. 10. Points



$$\begin{aligned} \tilde{\text{II}}_A^+ &= \text{II}_A^+ - \text{II}_A \\ \text{III}_A^+ &= U(\tilde{\text{II}}_A^+) \end{aligned}$$

FIG. 10. Same as Fig. 9 except for primary-1 back reaction. Note that the mapping of the reactive island II_A^+ forms the reactive island III_A^+ but whose symplectic area is less than $J_r(E)$ by $\text{Area}(\text{II}_A)$.

$Z \in \tilde{\text{II}}_A^+$ must map onto $\Sigma_A^+(E)$ for at least one additional mapping U . The symplectic area of $\tilde{\text{II}}_A^+$ must be preserved upon the mapping U , i.e., $\text{Area}(U(\tilde{\text{II}}_A^+)) = \text{Area}(\tilde{\text{II}}_A^+)$. Consistent with the previous notation, let $U(\tilde{\text{II}}_A^+)$ be denoted as III_A^+ . III_A^+ is still a reactive island, albeit one whose symplectic area is equal to $J_r(E) - \text{Area}(\text{II}_A)$. As before we let III_A be the overlap region between III_A^+ and II_A^- , $\text{III}_A = \text{III}_A^+ \cap \text{II}_A^-$. The solutions to Hamilton's equations of motion are unique thus requiring $\text{III}_A \cap \text{II}_A = \emptyset$. Assuming that $\text{III}_A \neq \emptyset$ then III_A is the region within II_A^- associated with secondary back reaction, i.e., the next most simple pathway to back reaction (in the present case of primary-1 back reaction, this would consist of two map iterations in $\Sigma_A^+(E)$). Then,

$$\text{Fraction of post-reactive motion} \\ \text{which undergoes secondary back} = \frac{\text{Area}(\text{III}_A)}{J_r(E)}. \quad (13)$$

reaction for a primary-1 system

Equivalently,

$$\begin{aligned} \text{Fraction of post-reactive} \\ \text{motion not undergoing} \\ \text{primary-1 back reaction} &= \frac{\text{Area}(\text{III}_A)}{J_r(E) - \text{Area}(\text{II}_A)} \\ \text{but undergoing} \\ \text{secondary back reaction} & \end{aligned} \quad (14)$$

The above analysis can be extended in a straightforward manner to obtain all higher order back reactive pathways and their respective fractions: The reactive island III_A^+ would be decomposed into III_A and its complement $\tilde{\text{III}}_A^+$. The region $\tilde{\text{III}}_A^+$ must map once again onto $\Sigma_A^+(E)$ forming the reactive island IV_A^+ and the overlap regions IV_A . The

overlap IV_A then contains within it the next most complex back reactive route, etc.. Carried out indefinitely, this procedure will generate overlap regions with II_A^- which are denoted by II_A, III_A, IV_A, \dots . These subregions quantify the fractional hierarchy of direct, secondary, tertiary, etc. back reaction. Let S_A^E be the ordered set of overlap regions with II_A^- at a total energy E ,

$$S_A^E = \{M_A = II_A^- \cap M_A^+, M = II, III, \dots\}. \quad (15)$$

Then S_A^E is the complete set of overlaps for back reaction from state A . This set is infinite but denumerable. It must also be true that, the sum of the symplectic areas of the members of S_A^E must equal the action of the periodic orbit τ ,

$$J_\tau(E) = \sum_{M=II}^{\infty} \text{Area}(M_A). \quad (16)$$

Thus, any trajectory within state A that eventually reacts onto state B can be viewed as a back reactor to some order.

2. States A and B bound

The discussion and results in the above subsection are applicable to systems with one bound and one unbound state, e.g., $H + Cl_2(v) \rightarrow (H \cdots Cl_2) \rightarrow Cl_2(v') + H$. However, our objective in this paper is to focus on the dynamics of conformational isomerization. Hence we now extend the discussion to the case where state B represent a bound conformer.

The generalization of the 2-map dynamics to include back reaction from conformer B is straightforward. Reactive islands generated by the initial extensions of $W_B^+(E)$ and $W_B^-(E)$ on Σ_B^- will also have a symplectic area equal to $J_\tau(E)$. The nature of both pre- and post-reactive motion in conformer B are the same as for conformer A . In particular motion cannot react from state B onto state A unless it enters the interior of the cylinder $W_B^-(E)$. Also post-reactive motion from conformer A must proceed through $W_B^+(E)$. The structure on the Σ_B^- map will take on similar characteristics as the map structure on Σ_A^+ . Following the convention for denoting reactive islands and overlap regions discussed for conformer A , we denote the reactive islands in $\Sigma_B^-(E)$ as II_B^\pm, III_B^\pm , etc. and the overlap regions with II_B^- as II_B, III_B, \dots with an obvious definition for the set S_B^E [cf. Eq. (15)].

In Fig. 11 we schematically display the 2-map dynamics for a symmetric two state system. All back reactive pathways can be quantified using the RI model above. In particular the fraction of motion undergoing each back reactive pathway from either conformer A or conformer B is precisely determined. Such detailed knowledge of the reaction dynamics will allow the construction of an accurate kinetic theory—which is the focus of the following section.

IV. REACTIVE ISLAND (RI) KINETIC THEORY

A. Two state conformational isomerization

In principle, an accurate microcanonical kinetic theory of two state isomerization should explicitly consider back reaction to all orders. However, since the sets S_A^E and S_B^E are infinite, such a detailed kinetic theory is not practical, indeed

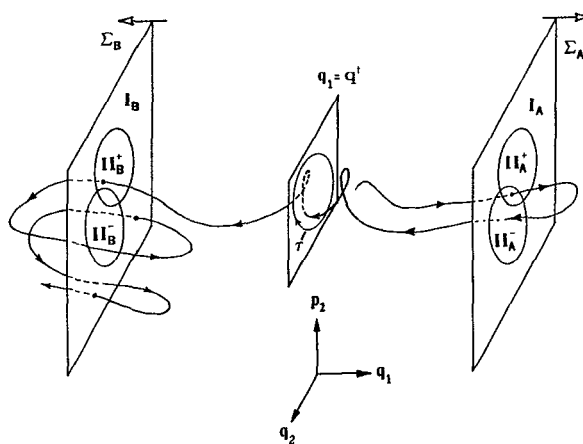
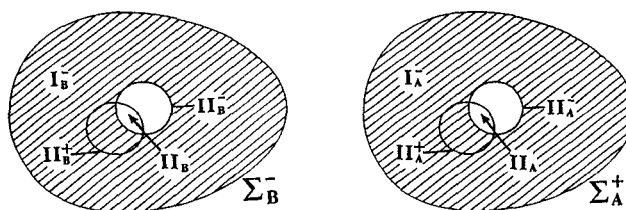


FIG. 11. Schematic drawing of 2-map dynamics for primary-1 (direct) back reaction. The sketch is in the same axis as that of Fig. 8. The curve winding through the figure represents a trajectory undergoing reaction.

not even necessary. Instead, a kinetic model based upon reactive islands is developed which explicitly includes back reaction for the first several members of S_A^E and S_B^E and the rest of the dynamics is treated as trapped \rightleftharpoons reactive motion.

1. Direct back reaction

A model which includes direct back reaction and trapped \rightleftharpoons reactive motion is the simplest 2-map RI kinetic model. Such a situation would result from the 2-map reactive island structure in Fig. 12. The mapping surfaces $\Sigma_A^+(E)$ and $\Sigma_B^-(E)$ are decomposed into the following subregions: $\Sigma_A^+(E)$ is subdivided into II_A^- and I_A^- , where I_A^- is the complement to the reactive island II_A^- , $I_A^- = \Sigma_A^+(E) - II_A^-$. Similar subregions are defined for state B . Assuming that all points $Z \in \Sigma_A^+(E)$ can undergo reaction, then a point $Z \in I_A^-$ must first map into II_A^- prior to reaction. (It is important to remember that a point $Z \in I_A^-$ cannot map onto $II_A \subset II_A^-$.) A symbolic representation of



$$I_A^- = \Sigma_A^+(E) - II_A^-$$

$$I_B^- = \Sigma_B^-(E) - II_B^-$$

FIG. 12. 2-map reactive island structure for the RI kinetic model which includes only primary-1 back reaction. Shaded region of the map is associated with "trapped" chaotic motion.

the mapping is given by the following simple diagram:

$$\begin{array}{ccc}
 II_B^- & \longrightarrow & I_A^- \\
 \uparrow & \searrow & \downarrow \\
 I_B^- & \longleftarrow & II_A^-
 \end{array} \quad (17)$$

where each arrow denotes a mapping U . In this mapping sequence the regions I_A^- and I_B^- are interpreted as those regions in $\Sigma_A^+(E)$ and $\Sigma_B^-(E)$ associated with trapped (i.e., not pre-reactive) motion. The diagram is read in the following way: A point $Z \in I_A^-$ will map either back onto I_A^- or II_A^- (i.e., $UZ \in I_A^-$ or II_A^-). In the former case UZ will remain trapped in $\Sigma_A^+(E)$, and in the latter case UZ will become pre-reactive. If $UZ \in II_A^-$ then UZ will react upon the next mapping U , ($U(UZ) \in II_B^-$). If $U^2Z \in I_B^-$ then it will be trapped within conformer B until it maps onto II_B^- . On the other hand, if $U^2Z \in II_B^-$ then it will again be pre-reactive.

A kinetic theory may be developed using the diagram above. To do so it is necessary to determine not only the mapping sequences, as given by the diagram, but one must also have a way of deciding where a point Z will map. For example, it is necessary to have some way of determining whether a $Z \in II_A^-$ will map onto either I_B^- or II_B^- . This may be accomplished by invoking a statistical model, which corresponds to the following approximation: In Sec. III A we discussed the various fractions for back reactive motion. We use these fractions to construct a statistical kinetic theory by using the following fundamental assumption: *The map dynamics generated by the mapping U is statistical.* By this statement we mean that the probability of a point Z mapping onto a subregion is equal to the fraction of motion mapping onto that subregion. In other words we assume that there are no internal dynamical correlations other than those required by the mapping sequences of reactive islands and area preservation. Similar statistical approximations to the dynamics have their precedent in the literature.^{41,46,51,67} Hence, within this approximation the mapping of a point Z will be probabilistic, depending only upon the relative areas of the subregions within the 2-map. Probability labels can now be placed on the mapping sequence in the diagram to give an RI kinetic mechanism,

$$\begin{array}{ccc}
 II_B^- & \xrightarrow{Q_1^A} & I_A^- \\
 P_{TR}^B \uparrow & P_1^A \searrow & P_1^B \downarrow P_{TR}^A \\
 I_B^- & \xleftarrow{Q_1^B} & II_A^-
 \end{array} \quad (18)$$

The probability of a pre-reactive trajectory from state B undergoing direct back reaction is P_1^A and the probability of it getting trapped (i.e., mapping onto I_A^-) is $Q_1^A = 1 - P_1^A$. These probabilities are given by [cf. Eq. (9)]

$$\begin{aligned}
 P_1^A &= \frac{\text{Area}(II_A^-)}{J_\tau(E)}, \\
 Q_1^A &= \frac{J_\tau(E) - \text{Area}(II_A^-)}{J_\tau(E)}.
 \end{aligned} \quad (19)$$

The probability for a point $Z \in I_A^-$ to map onto II_A^- (i.e., for trapped motion to become reactive) is P_{TR}^A . This probability is given by

$$P_{TR}^A = \frac{J_\tau(E) - \text{Area}(II_A^-)}{\text{Area}(I_A^-)}, \quad (20)$$

where $\text{Area}(I_A^-) = \text{Area}(\Sigma_A^+(E)) - J_\tau(E)$. Similar equations hold for P_1^B , Q_1^B , and P_{TR}^B .

With the kinetic mechanism and probabilities at hand, it is now simple to write down the associated kinetic equations. To do so we let the population of the subregion G upon the p th mapping U be denoted by $G(p)$ [$G(0)$ denotes initial populations], then

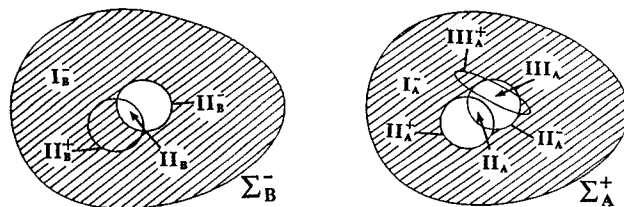
$$\begin{aligned}
 II_A^-(p) &= P_{TR}^A I_A^-(p-1) + P_1^A II_B^-(p-1), \\
 I_A^-(p) &= Q_{TR}^A I_A^-(p-1) + Q_1^A II_B^-(p-1), \\
 II_B^-(p) &= P_{TR}^B I_B^-(p-1) + P_1^B II_A^-(p-1), \\
 I_B^-(p) &= Q_{TR}^B I_B^-(p-1) + Q_1^B II_A^-(p-1),
 \end{aligned} \quad (21)$$

where $Q_{TR}^A = 1 - P_{TR}^A$, etc. This set of linearly coupled equations can be readily solved, cf. Sec. V.

The statistical approximation used above is, of course, an approximation to the true dynamics. Individual trajectories can be much more correlated with one another than assumed in this approximation—even if the dynamics is chaotic. However, from the perspective of an ensemble of trajectories, the statistical approximation appears to be, in most cases, excellent. In particular, non-RRKM effects can be accounted for and understood within the RI framework and the statistical approximation.

2. Direct + secondary back reaction

The kinetic model above includes only direct back reaction. It may, or may not be an accurate description of the reaction dynamics for a given Hamiltonian system at energy E . For example, it may turn out that secondary as well as primary back reaction from conformer A contributes significantly to the microcanonical reaction dynamics. The 2-map reactive island structure in Fig. 13 would yield a kinetic model which includes direct and secondary back reaction

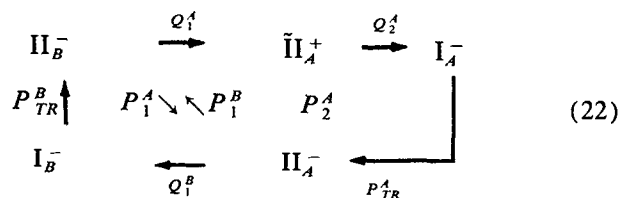


$$I_A^- = \Sigma_A^+(E) - II_A^- - II_A^+$$

$$I_B^- = \Sigma_B^-(E) - II_B^-$$

FIG. 13. 2-map reactive island structure for the RI kinetic model which includes primary-1 back reaction from conformer B and primary-1 plus secondary back reaction from conformer A . Shaded region of the map is associated with "trapped" chaotic motion.

from conformer *A* and only direct back reaction from conformer *B*. The kinetic mechanism is obtained by subdividing the map $\Sigma_A^+(E)$ into the regions II_A^+ and II_A^- and the complement subregion $\text{I}_A^- = \Sigma_A^+(E) - \text{II}_A^- - \text{II}_A^+$.⁶⁸ Using the ideas developed in Sec. III A 1 and invoking the statistical approximation, the kinetic mechanism is now given by



The probabilities P_1^A , P_{TR}^B , etc. have been previously discussed and given in Eqs. (19) and (20). The probabilities P_2^A and P_{TR}^A are given by

$$\begin{aligned}
 P_2^A &= \frac{\text{Area}(\text{III}_A)}{J_r(E) - \text{Area}(\text{II}_A)}, \\
 P_{TR}^A &= \frac{J_r(E) - \text{Area}(\text{II}_A) - \text{Area}(\text{III}_A)}{\text{Area}(\text{I}_A^-)}, \quad (23)
 \end{aligned}$$

where $\text{Area}(\text{I}_A^-) = \text{Area}(\Sigma_A^+(E)) - 2J_r(E) + \text{Area}(\text{II}_A)$ and $Q_2^A = 1 - P_2^A$.⁶⁹ The associated kinetic equations are easily constructed and are given by

$$\begin{aligned}
 \text{II}_A^-(p) &= P_{TR}^A \text{I}_A^-(p-1) + P_1^A \text{II}_B^-(p-1) \\
 &\quad + P_2^A \text{II}_A^+(p-1), \\
 \text{II}_A^+(p) &= Q_1^A \text{II}_B^-(p-1), \\
 \text{I}_A^-(p) &= Q_{TR}^A \text{I}_A^-(p-1) + Q_2^A \text{II}_A^+(p-1), \\
 \text{II}_B^-(p) &= P_{TR}^B \text{I}_B^-(p-1) + P_1^B \text{II}_A^-(p-1), \\
 \text{I}_B^-(p) &= Q_{TR}^B \text{I}_B^-(p-1) + Q_1^B \text{II}_A^-(p-1). \quad (24)
 \end{aligned}$$

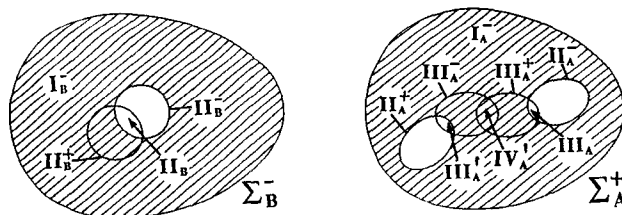
As before, these are a set of linearly coupled kinetic equations. This particular kinetic mechanism would only be considered for a molecular system where the two conformers are not equivalent. The same methods may be used to generalize the reactive island kinetic model to include any number of back reactions from conformers *A* and *B*.

3. Primary-2 back reaction

To this point, our discussion of the RI kinetic model has focused on systems that admit primary-1 (direct) back reaction. However, it is possible to encounter isomerization dynamics that does not admit primary-1 back reaction. Such a situation is not only possible but even likely at low excess energies. For example, consider the reactive island structure in Fig. 14. For this system direct back reaction from state *B* is possible, however direct back reaction from state *A* is not possible because $\text{II}_A^+ \cap \text{II}_A^- = \emptyset$. Note that III_A^- and II_A^+ are preimages of II_A^- and III_A^+ , respectively,

$$\begin{aligned}
 U(\text{III}_A^-) &= \text{II}_A^-, \\
 U(\text{II}_A^+) &= \text{III}_A^+. \quad (25)
 \end{aligned}$$

The preimage of the overlap III_A is $\text{III}_A' (= \text{II}_A^+ \cap \text{III}_A^-)$, i.e., $U(\text{III}_A') = \text{III}_A$. Since $\text{II}_A = \emptyset$, there is no primary-1 back reaction and the overlap region III_A is associated with primary-2 back reaction. There is also

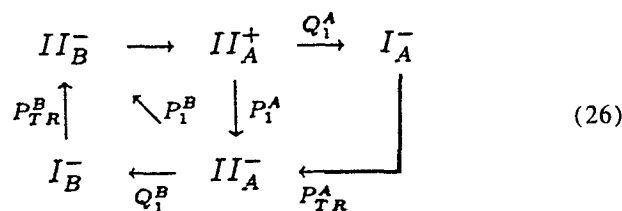


$$\text{I}_A^- = \Sigma_A^+(E) - \text{II}_A^- - \text{II}_A^+$$

$$\text{I}_B^- = \Sigma_B^-(E) - \text{II}_B^-$$

FIG. 14. Same as in Fig. 13, except the reactive island structure for conformer *A* admits primary-2 plus secondary back reaction (cf. Fig. 9). However, the kinetic mechanism discussed in the text [cf. Eq. (26)] ignores secondary back reaction (i.e., ignores the overlap region IV_A').

an overlap region $\text{IV}_A' = \text{III}_A^+ \cap \text{III}_A^-$. This overlap region is associated with secondary back reaction because of the following consideration: A point $Z \in \text{II}_B^-$ will map onto II_A^+ , whereupon it will map onto III_A^+ . If at this juncture Z lies within $\text{III}_A \subset \text{II}_A^-$ then Z will be pre-reactive (primary-2 back reaction), but if Z lies within $\text{IV}_A' \subset \text{III}_A^-$ then $U(\text{IV}_A') \subset \text{II}_A^-$ and will thus become pre-reactive upon the next mapping U , i.e., the next most simple pathway to back reaction—secondary back reaction. The simplest RI kinetic model for this system would ignore secondary and higher order back reactive pathways. The kinetic mechanism is then written as



where we use the convention that if an arrow does not have a probability label then the probability for that event is unity. The region I_A^- is given by $\text{I}_A^- = \Sigma_A^+(E) - \text{II}_A^- - \text{II}_A^+$ (cf. Fig. 14). The various probabilities are determined by Eqs. (19) and (20), and their conformer *B* counterparts. The area of I_A^- is now given by $\text{Area}(\text{I}_A^-) = \text{Area}(\Sigma_A^+(E)) - 2J_r(E)$. The kinetic equations are

$$\begin{aligned}
 \text{II}_A^-(p) &= P_{TR}^A \text{I}_A^-(p-1) + P_1^A \text{II}_A^+(p-1), \\
 \text{I}_A^-(p) &= Q_{TR}^A \text{I}_A^-(p-1) + Q_1^A \text{II}_A^+(p-1), \\
 \text{II}_A^+(p) &= \text{II}_B^-(p-1), \\
 \text{II}_B^-(p) &= P_{TR}^B \text{I}_B^-(p-1) + P_1^B \text{II}_A^-(p-1), \\
 \text{I}_B^-(p) &= Q_{TR}^B \text{I}_B^-(p-1) + Q_1^B \text{II}_A^-(p-1). \quad (27)
 \end{aligned}$$

The ideas presented above can, in a straightforward way, be extended to obtain a kinetic mechanism for any primary-*F* back reaction and any explicit number of back reactions. In the following section we discuss the generalization of RI kinetic theory to molecular systems undergoing unimolecular isomerization to multiple states.

B. Multi-state conformational isomerization

Once the basic concepts of the two state RI kinetic model are understood, their extension to include any number of conformational states is reasonably straightforward. As an example, consider the situation of three conformational states accessible at an excess energy ΔE . These states may correspond to a *trans-gauche-trans* isomerization of *n*-butane, or perhaps the isomerization of stilbene in its first excited electronic state.⁷⁰⁻⁷²

The discussion below will focus on the symmetric three state system in Fig. 15.⁷³ The reaction from one conformational state to another adjacent conformational state occurs over a potential energy barrier with a simple saddle, cf. Fig. 15. We assume that all periodic orbits τ about the saddle generate cylindrical manifolds. Two periodic orbits, one along each saddle of the potential, exist. Each periodic orbit, τ and τ' , will generate four phase space cylinders (cf. Fig. 7). The manner in which these cylinders overlap one another will determine the precise nature of the isomerization dynamics between the three conformers. Cylinders arising from the same periodic orbit will intersect one another along homoclinic orbits whereas cylinders arising from different periodic orbits will intersect one another along heteroclinic orbits. The manner in which the cylinders overlap one another will be quite complicated but can be unraveled using the same methods discussed for the two state system.

It is important for the *n*-map dynamics to capture all possible reactive motion. For the three state system under

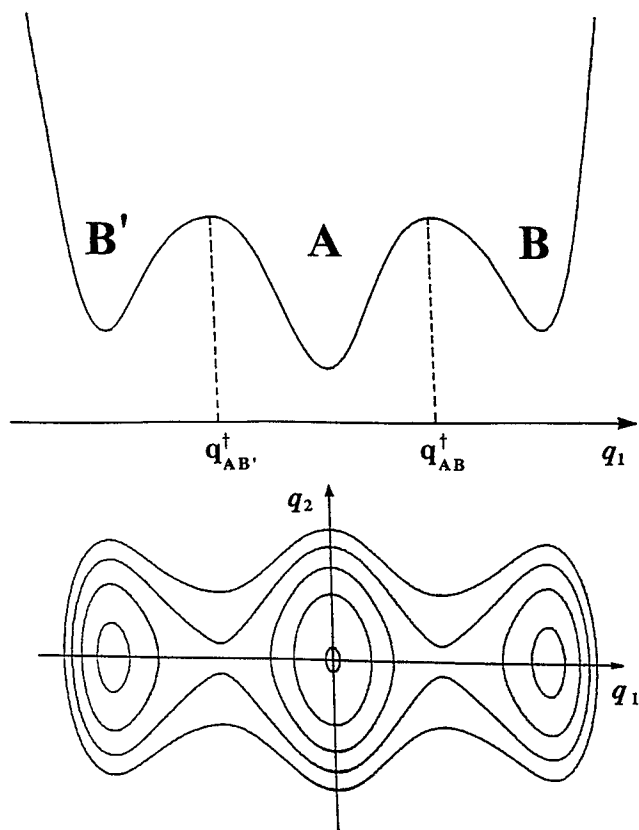


FIG. 15. Potential for three bound state conformational isomerization. Top: potential along reaction coordinate; bottom: potential contours.

consideration a 4-map will accomplish this goal. Let the dividing surface between conformers *A* and *B'* be at $q_{AB'}^\ddagger$ and the dividing surface between conformers *A* and *B* be at q_{AB}^\ddagger . We define the four maps as [cf. Eq. (4)],

$$\begin{aligned}\Sigma_B^+ &= \Sigma_{q_1}^+, & q_1 > q_{AB}^\ddagger \\ \Sigma_A^+ &= \Sigma_{q_1}^+, & q_{AB'}^\ddagger < q_1 < q_{AB}^\ddagger \\ \Sigma_A^- &= \Sigma_{q_1}^-, & q_{AB'}^\ddagger < q_1 < q_{AB}^\ddagger \\ \Sigma_{B'}^- &= \Sigma_{q_1}^-, & q_1 < q_{AB'}^\ddagger.\end{aligned}\quad (28)$$

The dynamics generated by the mapping *U* between these four Poincaré maps constitutes the 4-map dynamics. The construction of the RI kinetic model can now be accomplished using the concepts developed for the 2-map dynamics and kinetics.

Multi-state dynamics differs from the two state dynamics in that a hierarchy of *through* reactive pathways ($B' \rightarrow A \rightarrow B$) as well as back ($B' \rightarrow A \rightarrow B'$) pathways are possible and must be accounted for in a kinetic model. A 4-map RI structure which admits both *direct through* and *direct back* reaction is given in Fig. 16. The various reactive islands are labeled in this figure using the same definitions as developed for the two state model. Reactive islands with a subscript *B'* are generated from the cylinders originating at the barrier top about $q_{AB'}^\ddagger$. It should be noted that since direct through reaction is possible, then the area of III_{AB}^+ is equal to $J_\tau(E)$ minus the flux associated with direct through reaction [i.e., $\text{Area}(\text{II}_{AB'})$].

The kinetic mechanism corresponding to this 4-map RI structure as well as probabilities not explicitly discussed earlier are given in Fig. 17. While the mechanism for three state isomerization may appear more complex than for the two state case, in practice the distinction is purely technical; the basic concepts used to construct the model are the same.

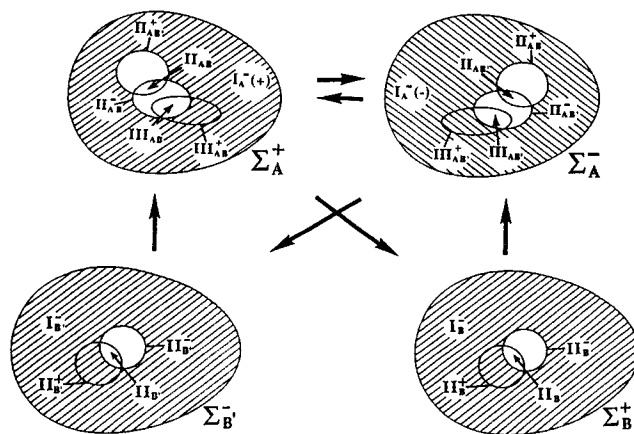
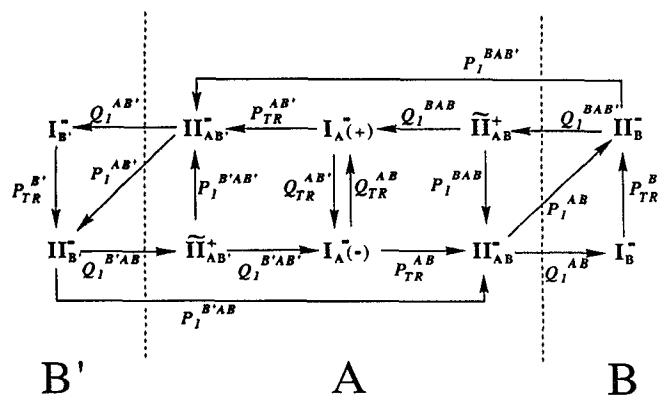


FIG. 16. A 4-map reactive island structure for the three state system in Fig. 15. This reactive island structure allows direct back reaction from conformers *A*, *B*, and *B'*. Direct through reaction is also allowed by this 4-map structure. The kinetic mechanism in Fig. 17 assumes that the shaded regions $I_A^\pm(\pm)$ are associated with chaotic trapped motion. These regions are given by $I_A^-(+) = \Sigma_A^+(E) - \text{II}_{AB}^- - \text{II}_{AB'}^+ + \text{II}_{AB}$, $I_A^-(-) = \Sigma_A^-(E) - \text{II}_{AB'}^- - \text{II}_{AB}^+ + \text{II}_{AB}$.



$$P_I^{B'AB} = \frac{\text{Area}(\text{II}_{AB})}{J_\tau(E)} = P_I^{BAB'}$$

$$P_I^{B'AB'} = \frac{\text{Area}(\text{III}_{AB})}{J_\tau(E) - \text{Area}(\text{II}_{AB})} = P_I^{BAB}$$

$$P_{TR}^{AB} = \frac{J_\tau(E) - \text{Area}(\text{II}_{AB} + \text{III}_{AB})}{\text{Area}(\text{I}_A(-))} = P_{TR}^{AB'}$$

FIG. 17. RI kinetic mechanism derived from the 4-map reactive island structure in Fig. 16.

The symmetric three state case discussed above is only an example of RI theory as applied to multiple conformers. Certain technical details such as the precise placement of the n mapping planes or even their definitions may vary for different molecular systems, but the fundamental notion that the cylindrical manifolds mediate conformational isomerization dynamics is generic.

In the following subsection we briefly consider a limiting case of the 2-map kinetic model which considers all motion as trapped \rightleftharpoons reactive.

C. Purely random 2-map kinetic model

As presented above, implementation of the RI n -map kinetic model requires information about overlaps between reactive islands. In this manner one can take into explicit account individual pathways to back reaction. However, one can imagine a kinetic model that treats all back reactive pathways on an equal footing—thus requiring a minimum of input for the kinetic model. We will call such a model the *purely random* n -map kinetic model. The advantage of this model is, of course, that it does not require any detailed information about the reactive island structure other than the symplectic area $J_\tau(E)$.

The purely random model assumes that the probability of a point $Z \in \Sigma_A^+$ undergoing reaction upon a mapping U is completely uncorrelated to its past or future.⁷⁴ Thus, in the purely random model there is only one probability to consider for each state, $P_{A \rightarrow B}$ and $P_{B \rightarrow A}$. It can be shown that the purely random model goes over to the standard transition state theory in the limit that the probabilities $P_{A \rightarrow B}$ and

$P_{B \rightarrow A}$ are much less than unity.⁷⁵ The kinetic mechanism for the purely random model is

$$\Sigma_B^- \rightleftharpoons \Sigma_A^+, \quad (29)$$

where

$$P_{B \rightarrow A} = \frac{J_\tau(E)}{\text{Area}(\Sigma_B^-(E))},$$

$$P_{A \rightarrow B} = \frac{J_\tau(E)}{\text{Area}(\Sigma_A^+(E))}. \quad (30)$$

If we let $\Sigma_A^+(p)$ and $\Sigma_B^-(p)$ denote the population within conformers A and B at the p th map iteration U^p , respectively, then the corresponding set of 2-map kinetic equations are

$$\Sigma_A^+(p) = Q_{A \rightarrow B} \Sigma_A^+(p-1) + P_{B \rightarrow A} \Sigma_B^-(p-1),$$

$$\Sigma_B^-(p) = P_{A \rightarrow B} \Sigma_B^-(p-1) + Q_{B \rightarrow A} \Sigma_A^+(p-1), \quad (31)$$

where the energy dependence of the populations has been left out for notational convenience.

D. Regular motion

We have considered the situation when every point Z is capable of both reacting and also becoming trapped, i.e., all of the dynamics is chaotic. However, both trapped and reactive regular motion can coexist with chaotic motion. Including the effects of regular motion on the reaction dynamics and RI kinetic theory is not difficult and is left for the appendix. In the following section we discuss the solution to the reactive island kinetic equations and focusing on the calculation of the reaction decay rate.

V. SOLUTION OF THE RI KINETIC EQUATIONS AND DECAY RATES

The set of linear RI kinetic equations can be solved by matrix methods which are, more or less, standard. Moreover, the solutions allow one to determine the relaxation rate for the reaction. To cast the equations in matrix form let \mathbf{N} be the column vector of all subpopulations. Furthermore, let components of \mathbf{N} be ordered such that the first K_A components are the subpopulations for conformer A , the next K_B components are the subpopulations within conformer B , etc. The vector $\mathbf{N}(p)$ is then the column vector of all subpopulations upon the p th mapping and $\mathbf{N}(0)$ represents the vector of initial populations. Let Θ be the real square matrix of probabilities that propagates $\mathbf{N}(p)$ upon one mapping U ,

$$\mathbf{N}(p+1) = \Theta \mathbf{N}(p). \quad (32)$$

Then,

$$\mathbf{N}(p) = \Theta^p \mathbf{N}(0). \quad (33)$$

Now, let Δ be the matrix of eigenvectors which diagonalizes Θ . We denote the diagonal matrix of eigenvalues $\lambda_1, \lambda_2, \dots$ as Λ . The matrix Θ is real but not symmetric. Therefore, both the eigenvectors and eigenvalues may be complex. One can write Eq. (33) as

$$\Delta^{-1} \mathbf{N}(p) = \Lambda^p \Delta^{-1} \mathbf{N}(0). \quad (34)$$

If we denote $\Delta^{-1} \mathbf{N}(p)$ by $\mathbf{R}(p)$, then Eq. (34) is written as $\mathbf{R}(p) = \Lambda^p \mathbf{R}(0)$. The eigenvector matrix Δ is in gen-

eral asymmetric and complex. In Ref. 45 we have shown how Δ^{-1} may be obtained through Θ and its transpose.

It is not difficult to show that the population of conformer A upon the p th mapping U^p is given by

$$A(p) = \sum_{j=1}^{K_{\text{TOT}}} a_j \lambda_j^p, \quad (35)$$

where K_{TOT} is the total number of components in \mathbf{N} . The coefficients a_j are expansion coefficients given by

$$a_j = R_j(0) \sum_{m=0}^{K_A} \Delta_{mj}, \quad (36)$$

where $R_j(0)$ is the j th component of $\mathbf{R}(0)$. Let us order the eigenvalues such that eigenvalues 1 to K_r are real and the rest are complex. Furthermore there will always be a unit eigenvalue, which just corresponds to conservation of total population; let this eigenvalue be λ_1 . It is then straightforward to show that

$$A(p) = a_1 + \sum_{j=2}^{K_r} a_j S_j^p e^{-k_j p} + 2 \sum_{j=K_r+1}^{K_{\text{TOT}}-1} [\text{Re}(a_j) \cos(\eta_j p) - \text{Im}(a_j) \sin(\eta_j p)] e^{-k_j p}, \quad (37)$$

where $S_j = \pm 1$ depending upon whether λ_j is positive or negative, η_j is the phase of the complex eigenvalue λ_j and the prime on the summation denotes a sum over indices $K_r + 1, K_r + 3, \dots, K_{\text{TOT}} - 1$. Note that a_j is real for $j = 1, 2, \dots, K_r$ and otherwise complex. The quantity k_j is interpreted as an exponential decay "rate" for the population R_j , i.e., $R_j(p) = e^{-k_j p} R_j(0)$ [cf. Eq. (34)], and is given by

$$k_j = -\ln(|\lambda_j|). \quad (38)$$

Equation (37) will yield the population of conformer A as a function of map iteration p . The detailed structure of the decay will clearly depend upon the initial population $\mathbf{N}(0)$. Note that $\mathbf{N}(0)$ discretizes the population. This leads us to an important point: The RI kinetic model divides the n -map into subregions. The dynamical flow between these subregions is guided by the RI kinetic equations. Thus, RI kinetic theory is a coarse grained representation of both the reaction dynamics and populations.

The decay rate for the overall reaction is obtained from the following purely qualitative considerations: Let us assume that a separation between a molecular time scale τ_{mol} and a relaxation time scale τ_{rxn} exists.^{24,26} In such a situation the long time population decay can be directly associated with the relaxation rate for the system. The relaxation time scale corresponds to the asymptotic decay of the population as it approaches equilibrium.⁷⁶ Note that the precise nature of the population decay is dependent upon the initial ensemble, however the asymptotic rate at which it decays is not. The RI theoretic prediction for τ_{rxn} can be extracted: According to the model, the long time relaxation of $A(p)$ will be exponential and be governed by the maximal eigenvalue whose norm is less than one⁷⁷ and whose expansion coefficient a_j is not equal to zero, λ_{max} , cf. Eq. (35). The exponential n -map relaxation "rate" will be given by

$$k_{\text{rxn}} = -\ln(|\lambda_{\text{max}}|). \quad (39)$$

Given k_{rxn} , the microcanonical relaxation rate τ_{rxn}^{-1} (in-

verse time units) is approximated by assuming that one can bridge it to the n -map rate k_{rxn} with the *average* time it takes a trajectory to undergo an n -map mapping,

$$\tau_{\text{rxn}}^{-1}(E) = k_{\text{rxn}}(E) T_{\text{rxn}}^{-1}(E). \quad (40)$$

T_{rxn} is the *average* n -mapping time which we will call the "characteristic reaction time" (see appendices B and C).

For two state isomerization it is given by (see Appendix B)

$$T_{\text{rxn}}(E) = \frac{\rho(E)}{\text{Area}(\Sigma_A^+(E)) + \text{Area}(\Sigma_B^-(E))}, \quad (41)$$

where $\rho(E)$ is the classical density of states $\text{Tr}(\delta(H - E))$. Note that Eq. (40) is independent of initial population conditions and constitutes the RI theory prediction for the relaxation rate. It should be emphasized that relating a dimensionless map "rate" to a temporal rate, as seen in Eq. (40), is a simplification. More generally, one can expect that the map and temporal dynamics are related by more than a simple scaling factor (see Appendix C). Nevertheless, approximations such as Eq. (40) have their precedent in the literature and have been demonstrated to be accurate.^{45-48,51} In Paper II, where temporal and map population decay rates are considered, Eq. (40) will be used to obtain the decay rate. It is easy to show that Eq. (40) is equivalent to the transition state theory prediction for the decay rate between two symmetric conformational states (Appendix C). The decay and decay rate of any initial conformer population (or combination of initial conformer populations) can be obtained using the equations above, which constitute the solution of the RI kinetic equations.

VI. DISCUSSION

In this paper we presented a formal development of the RI microcanonical kinetic theory of chemical reactions. We specifically focused on unimolecular isomerization. However, the basic ideas are applicable to unimolecular decomposition as well as bimolecular reactions. The development here differs significantly from earlier work^{53,54} in two important ways: (1) we focus attention on cylindrical manifolds in phase space as a global dynamical concept (i.e., not limited to unimolecular isomerization) and (2) the RI kinetic theory is developed with the concept of the n -map—on which the map dynamics between one conformer and another is not complicated by motion asymptotic to the transition state.

The formal development of the theory is based upon the existence of invariant manifolds with the geometry of simple cylinders embedded in phase space. The cylindrical manifolds rigorously mediate both pre- and post-reactive classical motion. Paper II of this series will present both numerical considerations and explicit calculations on a variety of model molecular systems representing conformational isomerization with two degrees of freedom. In Paper III we extend the concepts and applications to multidimensional molecular systems.

It is important to note that similar lines of thought have been addressed previously. In particular, Wigner, Hirshfelder, J. P. Davis, W. H. Miller, Pollak, Child, and Pechukas have considered the "recrossing" problem for bimolecular processes (see Sec. I). Somewhat more recently, Dumont and Brumer have used an ergodic theoretic approach to formalize the statistical assumptions in classical rate theories.⁶⁷ Their approach is based upon a decomposition of phase space into specific subsets. These subsets are defined in terms of the amount of *time* a trajectory will take to go from one point in configuration space to another. The isomerization rate theory presented in this paper considers subsets which are defined in terms of the *number of oscillations* in q_1 necessary to pass from one conformer to another. Another possible connection is with the recent work of Berne *et al.*²³ and Dumont^{27,67} who have dealt with the recrossing problem via the absorbing boundary method. In this method the fast "direct" component of the reaction dynamics is approximately separated from the "strong collision" component of the dynamics. These methods clearly have some ideas in common with RI theory and the possibility of a detailed connection between is intriguing and could form the basis of future work.

To generate explicit conformer population decays as well as extract rate constants for a specific molecular model, it is necessary to determine quantities such as $J_r(E)$ as well as the various overlap areas. One would like to calculate these quantities within a formal theoretical framework. Indeed recent developments suggest that this may be the case. For example the areas of so-called "turnstiles" may be obtained from the action differences of homoclinic orbits.⁷⁸⁻⁸⁰ Unfortunately the location of the homoclinic orbits is a numerically sensitive task and for this reason these formulas are not currently as practical as one would like. Furthermore, the extension of these equations to multidimensional systems is, at this time, numerically intractable since it is apparent that such formulas would require knowledge of a dense set of homoclinic orbits. On the other hand we have found that it is possible to obtain these areas using direct numerical procedures.⁵⁶

Aside from the extension to multidimensional systems, we see further development of RI theory along three principal fronts: (1) quantum mechanics,⁸¹ (2) theoretical modifications or extensions of the statistical assumption, and (3) application to realistic molecular systems. We have already conducted quantum mechanical numerical calculations on model two degree of freedom systems and have found that the quantum reaction dynamics is strongly influenced by the cylindrical manifolds.⁸² These preliminary results suggest that a quantum mechanical theory of cylindrical manifolds and reactive islands may be possible—perhaps along similar lines of thought as those of Miller.¹⁶ Another goal is to theoretically examine the statistical assumption and understand when it can be expected to succeed and fail, and if it fails to make the appropriate corrections. A final goal is to extend the calculations to consider canonical averages as well realistic molecular models in such a way that the calculations are more readily accessible. We believe that such a goal is possible since the evaluation of the overlaps required for the nu-

merical application of the theory may be computationally achieved in a straightforward way.⁵⁶

ACKNOWLEDGMENTS

We would like to thank Bruce Berne, Philip Pechukas, Eli Pollak and A. M. Ozorio de Almeida, and C. Clay Marston for useful conversations. This work was originally presented in its preliminary and final form in 1989 and 1990 at the 198th and 199th ACS meetings.

APPENDIX A

In the presentation of the RI kinetic theory we have assumed that the dynamics at energy E is chaotic over the entire energy surface. However, one generally expects chaotic and regular motion to coexist in dynamical systems. Two distinct types of regular motion are possible for systems capable of reaction over a potential barrier: (1) *trapped regular* and (2) *reactive regular* motion. Trapped regular motion evolves on an invariant torus which resides within a single conformational state, cf. $\Omega_{J_2}^A(E)$ of Fig. 3. Motion on such invariant tori will never react. On the other hand reactive regular motion evolves on a torus which spans more than one conformational state. Consequently reactive regular motion reacts periodically, cf. $\Omega_{J_2}^{AB}(E)$ of Fig. 3. The phase space measure of both types of invariant surfaces is finite and will thus give a finite contribution to the overall reaction dynamics. An accurate kinetic model must include the effect of both of these types of motion. We illustrate how regular motion may be included in the RI kinetic model by considering two state conformational isomerization.

First, since trapped regular motion cannot react then the overlap between the cylindrical manifolds and the region of phase space associated with trapped regular motion must be zero. On the other hand, the region of phase space associated with reactive regular motion must be contained completely within the cylindrical manifolds.

Let T_A be the region in $\Sigma_A^+(E)$ which contains trapped regular motion,

$$T_A = \{Z: Z \in \Sigma_A^+(E), U^{\pm n} Z \in \Sigma_A^+(E), n = 1, 2, 3, \dots, \infty\}. \quad (\text{A1})$$

Now, let R_A be the region in $\Sigma_A^+(E)$ which contains reactive regular motion and furthermore let this motion react on every mapping U ,

$$R_A = \{Z: Z \in \Sigma_A^+(E), U^{\pm n} Z \in \Sigma_B^-(E), n = 1, 3, 5, \dots, U^{\pm n} Z \in \Sigma_A^+(E), n = 2, 4, 6, \dots\}. \quad (\text{A2})$$

It follows that $R_A \subset \text{II}_A$, cf. Fig. 6(b). Inclusion of both types of regular motion in the RI kinetic model is simply accomplished: The region II_A is decomposed into R_A and $(\text{II}_A - R_A)$ and I_A^- is decomposed into T_A and $(\text{I}_A^- - T_A)$, i.e.,

$$\begin{aligned} \text{II}_A^- &\rightarrow \text{II}_A^- - R_A, \\ \text{I}_A^- &\rightarrow \text{I}_A^- - T_A. \end{aligned} \quad (\text{A3})$$

The simplest RI kinetic mechanism involving direct back-reaction is then written as

$$\begin{array}{ccc}
 II_B^- & \xrightarrow{Q_1^A} & I_A^- \\
 P_{TR}^B \uparrow & P_1^A \searrow & P_1^B \downarrow P_{TR}^A \\
 I_B^- & \xleftarrow{Q_1^B} & II_A^-
 \end{array}
 \quad (A4)$$

$$R_B \rightleftharpoons R_A$$

The probabilities P_1^A and P_{TR}^A are now given by

$$\begin{aligned}
 P_1^A &= \frac{\text{Area}(II_A^- - R_A)}{J_\tau(E) - \text{Area}(R_A)}, \\
 P_{TR}^A &= \frac{J_\tau(E) - \text{Area}(II_A^-)}{\text{Area}(I_A^-)},
 \end{aligned}
 \quad (A5)$$

where $\text{Area}(I_A^-) = \text{Area}(\Sigma_A^+(E)) - J_\tau(E) - \text{Area}(T_A)$. The resulting RI kinetic equations are

$$\begin{aligned}
 II_A^-(p) &= P_{TR}^A I_A^-(p-1) + P_1^A II_B^-(p-1), \\
 I_A^-(p) &= Q_{TR}^A I_A^-(p-1) + Q_1^A II_B^-(p-1), \\
 R_A(p) &= R_B(p-1), \\
 II_B^-(p) &= P_{TR}^B I_B^-(p-1) + P_1^B II_A^-(p-1), \\
 I_B^-(p) &= Q_{TR}^B I_B^-(p-1) + Q_1^B II_A^-(p-1), \\
 R_B(p) &= R_A(p-1).
 \end{aligned}
 \quad (A6)$$

The method of solution and calculation of the decay rate from these set of coupled linear equations is the same as that given in Sec. V. Similar considerations allow the inclusion of regular motion for any RI kinetic model.

APPENDIX B

In this appendix we derive Eq. (41) for $T_{\text{rxn}}(E)$, which is the average n -map mapping time for two state conformational isomerization. Throughout the derivation Fig. 18 should be carefully referenced. Consider the total density of states at energy E , which we denote as $\rho(E)$. We decompose $\rho(E)$ into the sum of the density of states of each conformer $\rho_A(E) + \rho_B(E)$. Now, consider the density of states encompassed by the cylinders $W_A^\pm(E)$ as they emerge from $\tau(E)$ and intersect the Poincaré surface $\Sigma_A^+(E)$ for the first time. Let the density of states so generated be designated $\rho_{W_A^\pm}(E)$. Similarly, let $\rho_{W_B^\pm}(E)$ be the classical density of states encompassed by the cylinders $W_B^\pm(E)$. With these definitions we can make the following decompositions:

$$\begin{aligned}
 \rho_A(E) &= \rho_{W_A^+}(E) + \rho_{W_A^-}(E) + \rho'_A(E), \\
 \rho_B(E) &= \rho_{W_B^+}(E) + \rho_{W_B^-}(E) + \rho'_B(E),
 \end{aligned}
 \quad (B1)$$

where $\rho'_A(E)$ and $\rho'_B(E)$ are the complement densities. The total density of states is written as

$$\begin{aligned}
 \rho(E) &= \rho_{W_A^+}(E) + \rho_{W_A^-}(E) + \rho_{W_B^+}(E) \\
 &\quad + \rho_{W_B^-}(E) + \rho_A(E)' + \rho_B(E)'.
 \end{aligned}
 \quad (B2)$$

Given these definitions, it is possible to derive the average n -map mapping time. First, let $\langle T \rangle_{A \rightarrow B}$ be the average time for points within II_A^- to map $\Sigma_A^+(E) \rightarrow \Sigma_B^-(E)$ in one 2-map mapping U . Binney *et al.*⁸³ have shown that this average time is related to the classical densities by

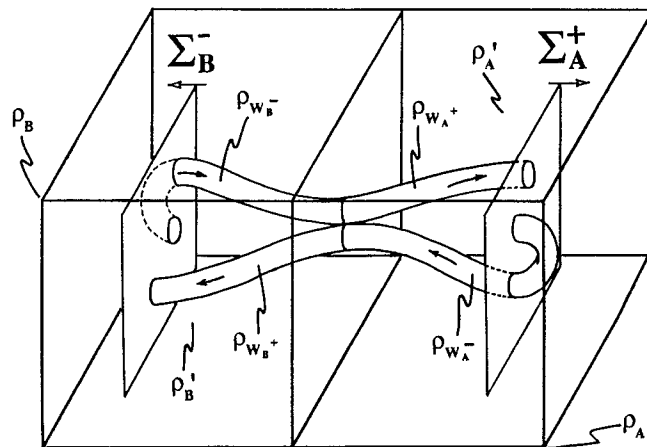


FIG. 18. A schematic diagram of the cylinders as they emerge from the $\tau(E)$ and intersect the Poincaré mapping planes Σ for the first time. The interior of the box represents the full volume of the system at an energy E , i.e., the total density of states at E , $\rho(E)$. The dividing plane represents the dividing surface between conformers A and B . All density of state labels ρ have an implicit dependence on E . The arrows within the cylinders represent the direction of the flow in phase space (see also Figs. 2, 5, 7, and 8).

$$\begin{aligned}
 \langle T \rangle_{A \rightarrow B} &= J_{\tau(E)}^{-1} \int_{\sigma} dp_2 dq_2 T(p_2, q_2), \quad \sigma = II_A^-, \\
 &= \frac{(\rho_{W_A^-}(E) + \rho_{W_B^+}(E))}{J_{\tau(E)}},
 \end{aligned}
 \quad (B3)$$

where the integral is taken over only those points $(p_2, q_2) \in II_A^-$ and $T(p_2, q_2)$ is the time it takes for a trajectory on some point $(p_2, q_2) \in \Sigma_A^+(E)$ to undergo a 2-map mapping U . Similarly, $\langle T \rangle_{B \rightarrow A}$ is given by

$$\begin{aligned}
 \langle T \rangle_{B \rightarrow A} &= J_{\tau(E)}^{-1} \int_{\sigma} dp_2 dq_2 T(p_2, q_2), \quad \sigma = II_B^- \\
 &= \frac{(\rho_{W_B^-}(E) + \rho_{W_A^+}(E))}{J_{\tau(E)}}.
 \end{aligned}
 \quad (B4)$$

Next, consider those points $(p_2, q_2) \in (\Sigma_A^+(E) - II_A^-)$. Since none of these points are in the reactive island II_A^- , they must all map back onto $\Sigma_A^+(E)$ for at least one 2-map mapping U . The average mapping time for these points will be given by

$$\begin{aligned}
 \langle T \rangle_{A \rightarrow A} &= \frac{\int_{\sigma} dp_2 dq_2 T(p_2, q_2)}{\text{Area}(\Sigma_A^+(E) - II_A^-)}, \quad \sigma = \Sigma_A^+(E) - II_A^- \\
 &= \frac{\rho_A^*(E)}{\text{Area}(\Sigma_A^+(E) - II_A^-)},
 \end{aligned}
 \quad (B5)$$

where $\rho_A^*(E)$ is the density of states associated with the points $(p_2, q_2) \in (\Sigma_A^+(E) - II_A^-)$. Similarly, for conformer B we have

$$\begin{aligned}
 \langle T \rangle_{B \rightarrow B} &= \frac{\int_{\sigma} dp_2 dq_2 T(p_2, q_2)}{\text{Area}(\Sigma_B^-(E) - II_B^-)}, \quad \sigma = \Sigma_B^-(E) - II_B^- \\
 &= \frac{\rho_B^*(E)}{\text{Area}(\Sigma_B^-(E) - II_B^-)},
 \end{aligned}
 \quad (B6)$$

If either (1) $\Sigma_A^+(E)$ is an attractive manifold,⁸⁴ or (2) the

dynamics over the entire energy surface is ergodic (i.e., dynamically indecomposable), then we can associate $\rho_A^*(E)$ with $\rho'_A(E)$ [cf. Eq. (B1)]. Similar conditions apply to associate $\rho_B^*(E)$ with $\rho'_B(E)$. Herein, let us assume either (1) or (2) or both of the above conditions are met by the Poincaré surfaces and/or the dynamics. Substitution of Eqs. (B3)–(B6) into Eq. (B2) yields

$$\begin{aligned} \rho(E) = & J_{\tau(E)} \langle T \rangle_{A \rightarrow B} + J_{\tau(E)} \langle T \rangle_{B \rightarrow A} \\ & + \text{Area}(\Sigma_A^+(E) - \Pi_A^-) \langle T \rangle_{A \rightarrow A} \\ & + \text{Area}(\Sigma_B^-(E) - \Pi_B^-) \langle T \rangle_{B \rightarrow B}. \end{aligned} \quad (\text{B7})$$

Thus, the density of states is a weighted sum of the individual average n -map mapping times. Note that,

$$\begin{aligned} \text{Area}(\Sigma_A^+ + \Sigma_B^-) = & 2J_{\tau(E)} + \text{Area}(\Sigma_A^+(E) - \Pi_A^-) \\ & + \text{Area}(\Sigma_B^-(E) - \Pi_B^-). \end{aligned} \quad (\text{B8})$$

Therefore, if we divide Eq. (B7) by the total n -map area, $\text{Area}(\Sigma_A^+(E) + \Sigma_B^-(E))$, then the right-hand-side of the resulting equation is just the average n -map mapping time $T_{\text{rxn}}(E)$ and we have

$$T_{\text{rxn}}(E) = \frac{\rho(E)}{\text{Area}(\Sigma_A^+(E) + \Sigma_B^-(E))}. \quad (\text{B9})$$

The derivation above can be extended to any n -map.

APPENDIX C

In this appendix we make use of the results in Appendix B to relate the microcanonical transition state theory value for the decay rate $(\tau_{\text{rxn}}(E))_{\text{TST}}^{-1}$ to the characteristic reaction time T_{rxn} . We will focus on two state conformational isomerization, but the ideas can be extended in a straightforward

manner to several conformers. According to transition state theory, the microcanonical decay rate between two conformers is given by

$$(\tau_{\text{rxn}}(E))_{\text{TST}}^{-1} = \frac{J_{\tau}(E)}{\chi_A \chi_B \rho(E)}, \quad (\text{C1})$$

where $\chi_A = \rho_A \rho^{-1}$ and $\chi_B = \rho_B \rho^{-1}$, i.e., the microcanonical mole fractions. If conformer A and conformer B are symmetric, then $\text{Area}(\Sigma_A^+(E)) = \text{Area}(\Sigma_B^-(E))$ and

$$\chi_A \chi_B = \frac{1}{4} = \frac{\text{Area}(\Sigma_A^+(E)) \text{Area}(\Sigma_B^-(E))}{\text{Area}^2(\Sigma_A^+(E) + \Sigma_B^-(E))}. \quad (\text{C2})$$

In this case Eq. (41) is an exact relation for $(\tau_{\text{rxn}}(E))_{\text{TST}}^{-1}$ with $k_{\text{rxn}} = P_{A \rightarrow B} + P_{B \rightarrow A}$ (see below). However, for the more general situation where conformers A and B are not symmetric one must relate phase space volumes to map areas.

A fundamental assumption of transition state theory, as applied to conformational isomerization, is that the time scale in which motion recrosses the dividing surface is long relative that of reaction. A necessary but not sufficient condition for this condition to accurately represent the underlying dynamics is that $\text{Area}(\Sigma_A^+(E)) \gg J_{\tau}(E)$ (i.e., the reactive island is very small). A similar condition holds for $\text{Area}(\Sigma_B^-(E))$. We will henceforth assume this to be the case. Furthermore, we will assume conditions (1) and/or (2) (i.e., attractive manifold or ergodicity) cited in Appendix B. Equations (B5) and (B6) can now be written as

$$\begin{aligned} \rho_A(E) & \approx \langle T \rangle_{A \rightarrow A} \text{Area}(\Sigma_A^+(E)), \\ \rho_B(E) & \approx \langle T \rangle_{B \rightarrow B} \text{Area}(\Sigma_B^-(E)). \end{aligned} \quad (\text{C3})$$

Equation (C3) can be used to write

$$\chi_A \chi_B = \frac{\rho_A \rho_B}{\rho^2} \approx \frac{\langle T \rangle_{A \rightarrow A} \langle T \rangle_{B \rightarrow B} \text{Area}(\Sigma_A^+(E)) \text{Area}(\Sigma_B^-(E))}{(\langle T \rangle_{A \rightarrow A} \text{Area}(\Sigma_A^+(E)) + \langle T \rangle_{B \rightarrow B} \text{Area}(\Sigma_B^-(E)))^2}. \quad (\text{C4})$$

The average times $\langle T \rangle_{A \rightarrow A}$ and $\langle T \rangle_{B \rightarrow B}$ can be physically interpreted as the average *period* of oscillation of the reaction coordinate q_1 in conformers A and B , respectively. Therefore, if the average period of oscillation of conformer A is about the same as the average period of oscillation of conformer B , then one can write

$$\chi_A \chi_B \approx \frac{\text{Area}(\Sigma_A^+(E)) \text{Area}(\Sigma_B^-(E))}{\text{Area}^2(\Sigma_A^+(E) + \Sigma_B^-(E))}. \quad (\text{C5})$$

Equation (C5) allows us to relate the decay rate to the characteristic reaction time,

$$(\tau_{\text{rxn}}(E))_{\text{TST}}^{-1} \approx \frac{P_{A \rightarrow B} + P_{B \rightarrow A}}{T_{\text{rxn}}}, \quad (\text{C6})$$

where $P_{A \rightarrow B}$ and $P_{B \rightarrow A}$ are given by Eq. (30).

¹ H. S. Johnston, *Gas Phase Reaction Rate Theory* (Roland, New York, 1966).

² W. Forst, *Theory of Unimolecular Reactions* (Academic, New York, 1973).

³ W. C. Gardiner, *Rates and Mechanisms of Chemical Reactions* (Benjamin,

New York, 1969).

⁴ S. Glasstone, K. Laidler, and H. Eyring, *The Theory of Rate Processes* (McGraw-Hill, New York, 1941).

⁵ E. E. Nikitin, *Theory of Elementary Atomic and Molecular Processes* (Clarendon, Oxford, 1974).

⁶ H. Eyring, *J. Chem. Phys.* **3**, 107 (1934).

⁷ E. Wigner, *J. Chem. Phys.* **5**, 720 (1937); J. O. Hirschfelder and E. Wigner, *ibid.* **7**, 616 (1939).

⁸ H. A. Kramers, *Physica* **4**, 284 (1940).

⁹ R. A. Marcus, *J. Chem. Phys.* **20**, 359 (1952).

¹⁰ G. M. Wieder and R. A. Marcus, *J. Chem. Phys.* **37**, 1835 (1962).

¹¹ R. A. Marcus, *Ber. Bunsenges. Phys. Chem.* **92**, 209 (1988).

¹² J. C. Keck, *J. Chem. Phys.* **32**, 1035 (1960).

¹³ J. C. Light, *J. Chem. Phys.* **40**, 3221 (1964).

¹⁴ P. Pechukas and J. C. Light, *J. Chem. Phys.* **42**, 3281 (1965).

¹⁵ J. C. Light, *Discuss. Faraday Soc.* **44**, 14, (1967).

¹⁶ W. H. Miller, *J. Chem. Phys.* **61**, 1823 (1974).

¹⁷ E. Pollak and P. Pechukas, *J. Chem. Phys.* **69**, 1218 (1978).

¹⁸ P. Pechukas and E. Pollak, *J. Chem. Phys.* **71**, 2062 (1979).

¹⁹ E. Pollak and M. S. Child, *J. Chem. Phys.* **73**, 4273 (1980).

²⁰ E. Pollak, *Theory of Chemical Reaction Dynamics*, Volume III, edited by M. Baer (CRC, Boca Raton, 1985).

²¹ J. A. Montgomery, Jr., D. Chandler, and B. J. Berne, *J. Chem. Phys.* **70**, 4056 (1979).

²² R. F. Grote and J. T. Hynes, *J. Chem. Phys.* **77**, 3736 (1982).

²³ J. E. Straub, M. Borkovec, and B. J. Berne, *J. Chem. Phys.* **89**, 4833 (1988).

- ²⁴ D. Chandler, *J. Chem. Phys.* **68**, 2959 (1978).
- ²⁵ J. T. Hynes, *Theory of Chemical Reaction Dynamics*, edited by M. Baer (CRC, Boca Raton, Florida, 1985).
- ²⁶ B. J. Berne, *Multiple Time Scales*, edited by J. U. Brackbill and B. I. Cohen (Academic, New York, 1985).
- ²⁷ R. S. Dumont, *J. Chem. Phys.* **91**, 6839 (1989).
- ²⁸ D. G. Truhlar, W. L. Hase, and J. T. Hynes, *J. Phys. Chem.* **87**, 2664 (1983).
- ²⁹ P. Pechukas, *Dynamics of Molecular Collisions, Part B*, edited by W. H. Miller (Plenum, New York, 1976).
- ³⁰ K. V. Reddy and M. J. Berry, *Chem. Phys. Lett.* **52**, 111 (1977).
- ³¹ D. W. Chandler, W. E. Farneth, and R. N. Zare, *J. Chem. Phys.* **77**, 4447 (1982).
- ³² J. A. Syage, P. M. Felker, and A. H. Zewail, *J. Chem. Phys.* **81**, 2233 (1984).
- ³³ J. A. Syage, P. M. Felker, and A. H. Zewail, *J. Chem. Phys.* **81**, 4706 (1984).
- ³⁴ D. B. Borchartd and S. H. Bauer, *J. Chem. Phys.* **85**, 4980 (1986).
- ³⁵ S. H. Courtney, M. W. Balk, L. A. Philips, S. P. Webb, D. Yang, D. H. Levy, and G. R. Fleming, *J. Chem. Phys.* **89**, 6697 (1988).
- ³⁶ D. L. Bunker, *J. Chem. Phys.* **40**, 1946 (1963).
- ³⁷ D. L. Bunker and M. Pattengill, *J. Chem. Phys.* **48**, 772 (1968).
- ³⁸ W. L. Hase, *Dynamics of Molecular Collisions, Part B*, edited by W. H. Miller (Plenum, New York, 1976).
- ³⁹ L. Gene Spears, Jr. and J. S. Hutchinson, *J. Chem. Phys.* **88**, 240 (1988); **88**, 250 (1988).
- ⁴⁰ R. J. Wolf, *J. Chem. Phys.* **72**, 316 (1979); **73**, 3779 (1980); **75**, 3809 (1981).
- ⁴¹ W. H. Miller, *J. Chem. Phys.* **65**, 2216 (1976).
- ⁴² J. P. Davis, *J. Chem. Phys.* **71**, 5206 (1979).
- ⁴³ J. P. Davis, *J. Chem. Phys.* **73**, 2010 (1980).
- ⁴⁴ J. P. Davis, *J. Chem. Phys.* **76**, 1754 (1982).
- ⁴⁵ B. C. Garrett and D. G. Truhlar, *J. Phys. Chem.* **83**, 1052 (1979); **84**, 805 (1980); **85**, 1569 (1981); B. C. Garrett and D. G. Truhlar, *J. Chem. Phys.* **74**, 1853 (1982).
- ⁴⁶ M. J. Davis, *J. Chem. Phys.* **83**, 1016 (1985).
- ⁴⁷ M. J. Davis and S. K. Gray, *J. Chem. Phys.* **84**, 5389 (1986).
- ⁴⁸ R. T. Skodje and M. J. Davis, *J. Chem. Phys.* **88**, 2429 (1988).
- ⁴⁹ M. J. Davis, *J. Chem. Phys.* **86**, 3978 (1987).
- ⁵⁰ N. De Leon and B. J. Berne, *J. Chem. Phys.* **75**, 3495 (1981); B. J. Berne, *Chem. Phys. Lett.* **107**, 131 (1984).
- ⁵¹ S. K. Gray and S. A. Rice, *J. Chem. Phys.* **86**, 2020 (1987).
- ⁵² R. De Vogelaere and M. Boudart, *J. Chem. Phys.* **23**, 1236 (1955).
- ⁵³ C. Clay Marston and N. De Leon, *J. Chem. Phys.* **91**, 3392 (1989).
- ⁵⁴ N. De Leon and C. Clay Marston, *J. Chem. Phys.* **91**, 3405 (1989).
- ⁵⁵ A. Ozorio de Almeida, N. De Leon, Manish A. Mehta, and C. Clay Marston, *Physica D* **46**, 265 (1990).
- ⁵⁶ N. De Leon, Manish A. Mehta, and R. Q. Topper, *J. Chem. Phys.* **94**, 8329 (1991).
- ⁵⁷ N. De Leon, Manish A. Mehta, and R. Q. Topper (in preparation).
- ⁵⁸ V. I. Arnold, *Mathematical Methods of Classical Mechanics* (Springer-Verlag, New York, 1978).
- ⁵⁹ A. M. Ozorio de Almeida, *Hamiltonian Systems: Chaos and Quantization* (Cambridge University, Cambridge, England, 1988).
- ⁶⁰ S. Wiggins, *Global Bifurcations and Chaos* (Springer-Verlag, New York, 1988).
- ⁶¹ A. J. Lichtenberg and M. A. Lieberman, *Regular and Stochastic Motion* (Springer-Verlag, New York, 1983).
- ⁶² For systems capable of undergoing bound state isomerization $\tau(E)$ will generally turn out to be repulsive. However, it is conceivable that $\tau(E)$ can, at some E , become attractive. The methods in this paper are not immediately applicable to this case; however, new periodic orbits which are repulsive are expected to emerge. These new periodic orbits will generate cylindrical manifolds.
- ⁶³ H. Poincaré, *Les Méthodes Nouvelles de la Mécanique Céleste*, Tome III (Gauthier-Villars, Paris, 1899); A translation in English is available: NASA technical translation, NASA TT F-452 (Dover, New York, 1957).
- ⁶⁴ By stating that $\Omega_{\lambda}^{\pm}(E)$ is compact we mean that the set of points $Z \in \Gamma$ that lie on $\Omega_{\lambda}^{\pm}(E)$ is both closed and bounded. The set of points Z on the cylindrical manifolds $W_{\lambda}^{\pm}(E)$ is bounded but not closed. Therefore the cylinders $W_{\lambda}^{\pm}(E)$ are not compact.
- ⁶⁵ For $N = 2$ the cylinders will not necessarily visit all regions of phase space where the dynamics is chaotic. For $N > 2$, regular motion no longer bounds regions of phase space where the dynamics is chaotic. Hence, unless additional dynamical restrictions exist, these regions are accessible to the cylinders.
- ⁶⁶ As $W_{\lambda}^{\pm}(E)$ extends out into phase space and undergoes deformations, the concept of "interior" and "exterior" begins to lose its physical meaning.
- ⁶⁷ R. S. Dumont and P. Brumer, *J. Phys. Chem.* **90**, 3509 (1986); R. S. Dumont, *J. Chem. Phys.* **91**, 4679 (1989).
- ⁶⁸ This notation differs slightly from that of Ref. 46.
- ⁶⁹ In the language of statistics one would refer to the probabilities P_1, P_2 , etc. as conditional probabilities: P_1 is the probability that a trajectory will undergo primary back reaction, P_2 is the probability that a trajectory will undergo secondary back reaction given that it has not undergone primary back reaction, etc.
- ⁷⁰ R. A. Scott and H. A. Scheraga, *J. Chem. Phys.* **44**, 3054 (1966).
- ⁷¹ J. P. Ryckart and A. Bellemans, *Chem. Phys. Lett.* **30**, 23 (1975).
- ⁷² J. A. Syage, P. M. Felker, and A. H. Zewail, *J. Chem. Phys.* **81**, 4685 (1984).
- ⁷³ We note that there is a close analogy between the periodic orbit structure for this three bound state system and the periodic orbit structure discussed by Pollak, Pechukas, and Child (PPC) for collinear bimolecular reactions. In particular, by symmetry there exists a periodic orbit along q_2 at the bottom of the well in state A . In the language of PPC this periodic orbit would be called "attractive" whereas the two τ periodic orbits on either side of it would be called "repulsive." Hence, the three state isomerization dynamics is mediated by the repulsive-attractive-repulsive character of the periodic orbits in much the same manner as bimolecular reaction dynamics.
- ⁷⁴ M. C. Wang and G. E. Uhlenbeck, *Noise and Stochastic Processes*, edited by N. Wax (Dover, New York, 1954).
- ⁷⁵ This is because $-\ln(1 - P_{A \rightarrow B} - P_{B \rightarrow A})$ approximately equals $P_{A \rightarrow B} + P_{B \rightarrow A}$ in the limit that $P_{A \rightarrow B}$ and $P_{B \rightarrow A}$ are much less than unity.
- ⁷⁶ The equilibrium population of each individual subpopulation can be easily obtained by recognizing that the n -map dynamics must obey detailed balance (i.e., due to microscopic reversibility). Using detailed balance one finds that the population of a given subregion is directly proportional to its symplectic area. The equilibrium distribution on all maps is thus uniform.
- ⁷⁷ B. Widom, *J. Chem. Phys.* **55**, 44 (1971).
- ⁷⁸ R. S. MacKay, J. D. Meiss, and I. C. Percival, *Physica D* **13**, 55 (1984).
- ⁷⁹ R. S. MacKay, J. D. Meiss, and I. C. Percival, *Physica D* **27**, 1 (1987).
- ⁸⁰ R. S. MacKay and J. D. Meiss, *J. Phys. A* **19**, L225 (1986).
- ⁸¹ D. C. Chatfield, R. S. Friedman, D. G. Truhlar, B. C. Garrett, and D. W. Schwenke, *J. Am. Chem. Soc.* **113**, 486 (1991).
- ⁸² Manish A. Mehta and N. De Leon (unpublished results).
- ⁸³ J. Binney, O. E. Gerhard, and P. Hut, *Mon. Not. Roy. Astron. Soc.* **215**, 59 (1985).
- ⁸⁴ If the boundary of $\Sigma_{\lambda}^{\pm}(E)$ is a periodic orbit then it can be either attractive or repulsive (Ref. 73). We will denote an attractive periodic orbit as an "attractive manifold," independent of whether it is stable or unstable. This terminology becomes especially useful when the system has three or more degrees of freedom (Ref. 57).